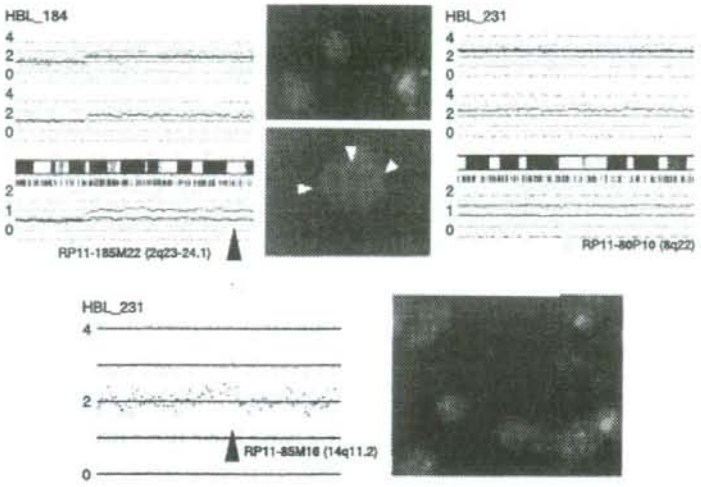

Fig. 3. Representative results of array analysis of hepatoblastoma (HBL) samples (HBL_184 and HBL_231). Fluorescent *in situ* hybridization analysis with BAC probes confirmed the detected changes. We detected three signals from chromosomes 2q and 8q. At the high-amplification region of chromosome 14q, three and more signals were detected.

Table 2. Chromosomal aberrations in 17 primary hepatoblastoma (HBL) samples

Sample	Copy number gain	Copy number loss	Uniparental disomy
HBL_4	1q, 2q34, 5p13.1, 17q23.3-qter	3p13-pter, 3q13.11, 6q14.1-qter, 11q23.1-qter	Not detected
HBL_7	1q, 2, 8, 14q11.2, 20	not detected	11p15.4-pter
HBL_8	7q34	not detected	Not detected
HBL_9	1q, 2q14.1-qter, 6p, 7, 14q11.2	6p12.1, 9p21.1	Not detected
HBL_12	8q11.23, 10q21.3, 10q26.13, 14q11.2, 22q13.31	7q35	Not detected
HBL_14	2p16.3-p22.3, 2p23.1, 2q11.2-q14.1, 2q33.1-q34, 3p21.33-p22.1, 3p24.2, 3p25.1, 3p25.2, 4q32.2-q32.3, 5p13.2, 6q14.3-q16.1, 7q, 11p15.1, 10p13-pter, 11q22.2-q22.3, 12p13.2-pter, 14q23.3-q31.1, 15q22.31-q26.2, 16p12.3, 20p11.23	1q31.1-qter, 2p12-14, 3, 4q, 5p14.1-pter, 5q32-qter, 6p12.13-pter, 6q11.1, 6q25.1-qter, 8, 9, 12p11.1-13.1, 17q24.3, 18p11.21-11.32, 18q21.1-qter, 19, 22	Not detected
HBL_22	Not detected	Not detected	Not detected
HBL_27	1q, 2q24.2-24.3, 7q34, 14q11.2	4q32.3-qter, 16p12.1	Not detected
HBL_28	3p26.1, 7q34, 14q11.2, 20	2p24.1	11p14.3-pter
HBL_34	1q, 2, 7q34, 14q11.2, 17	4q34.1-qter	Not detected
HBL_36	1q32.1-qter	1p13.3-pter, 4q21.22-qter, 5p13.1	Not detected
HBL_37	1q, 2, 5, 6, 7q34, 8, 10, 12, 14, 14q11.2, 15, 16q22.1-pter, 17, 19, 20	Not detected	11p15.2-pter, 16q22.2-qter
HBL_184	2q14.2-qter, 3p24.3, 4q33, 10p14, 11p14.3, 14q11.2	Not detected	Not detected
HBL_185	6p, 21q21.2	Not detected	Not detected
HBL_231	8, 14q11.2, 19, 20	Not detected	11p15.4-pter
HBL_246	1q, 2, 5, 6, 8, 10, 12, 13, 16, 17, 19, 20, 21, 22	Not detected	4, 9
HBL_250	Not detected	Not detected	Not detected

CN gains at 14q11.2 (Fig. 3). Further, in RQ-PCR analysis, the CN gain of *EphB6* and *DAD1* was evident in all samples that showed high-grade amplification in SNP array (data not shown). Other high-grade amplifications are listed in Table 3. The size of these amplicons was typically less than 1 Mb, and the possible genes present in these regions are summarized in the same table. All these candidate genes, except *MMP7*, have not been reported previously with regard to HBL.[33]

Homozygous deletions are also of particular interest because they may indicate a tumor suppressor gene. However, homozygous deletions were not identified in any sample.

CN neutral LOH (UPD). LOH can be more sensitively detected with the CNAG/AsCNAR algorithms by evaluating the allele-specific CN than from the grossly reduced heterozygous SNP calls, particularly when the SNP shows no CN losses. The UPD regions were identified in five of the 17 samples. In four samples (HBL_7, HBL_28, HBL_37, and HBL_231), 11p15 was the common UPD region (Fig. 4a). Other UPD regions were observed within chromosomes 4, 9, and 16q22 (Table 2). The candidate target genes that map to the UPD region located within 11p15 include *IGF2* and *H19*. Methylation-specific PCR analysis was performed for the four HBL samples having UPD within 11p15 to identify the origin of the amplified allele. The methylation status of the differential methylated region (DMR) of *H19* is shown in Fig. 4b. Hypermethylation of the *H19* DMR was detected in all HBL samples having UPD within 11p15; however, normal lymphocyte DNA showed the mosaic methylation pattern. In general, the *H19* DMR is hypermethylated on the paternal allele

© 2008 Japanese Cancer Association

Table 3. High-grade amplifications in hepatoblastoma (HBL) samples

Cytoband	Implicated region (base pairs)		Candidate target genes in the region
	Start–end	Size	
2q34	211 193 864–212 239 181	1 045 318	*ErbB4*
3p25.2	11 888 124–12 876 175	988 052	*RAF1*
7q34	141 721 559–142 076 238	354 680	*EphB6*
11q22.2-q22.3	101 394 973–102 830 195	1 435 223	*MMP1, 7, 20*
14q11.2	21 426 631–22 130 392	703 762	*DAD1*

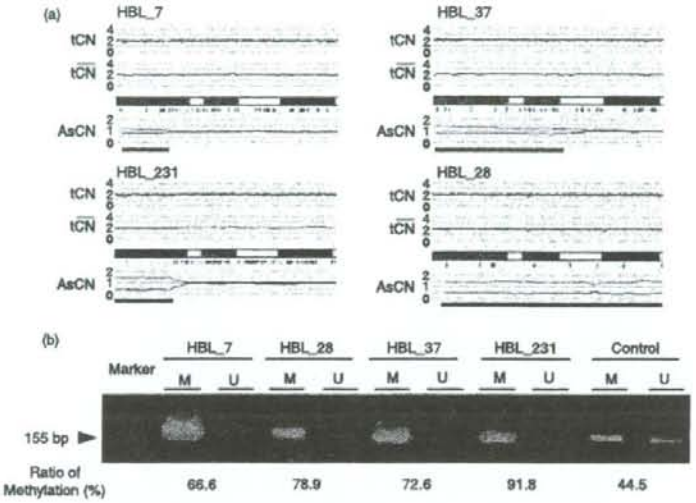

Fig. 4. (a) Copy numbers (CN) of chromosome 11p in four hepatoblastoma (HBL) samples with uniparental disomy (UPD). Although complete CN alterations are not observed, UPD is clearly predicted based on the allele-specific CN alterations (green lines). (b) Methylation-specific polymerase chain reaction (PCR) analysis of the *H19* differential methylated region (DMR). Modified DNA was amplified with primer pairs for methylated and unmethylated complete sequences of the *H19* DMR. *H19* DMR hypermethylation was detected in all HBL samples; however, normal lymphocyte DNA exhibited the mosaic methylation pattern. The results of quantitative real-time methylation-specific PCR analysis are shown below the image depicting the results of electrophoresis.

and hypomethylated on the maternally expressed allele in humans. This indicates that the UPD within this region is considered to be derived from the paternal allele. Furthermore, a low expression level of the non-methylated allele was also observed; methylation-specific RQ-PCR analysis revealed that the ratio of the methylation status ranged from 66.6% to 91.8%.

Expression analyses using RQ-RT-PCR. In order to examine the impact of the abovementioned amplifications and UPD on gene expression, we measured the expression levels of four genes (*DAD1*, *ErbB4*, *IGF2*, and *H19*) through RQ-RT-PCR (Fig. 5). Normal liver total RNA served as the non-neoplastic reference and control. HBL_184 and HBL_231 for which RNA were available showed a high expression of the *ErbB4* gene. However, the expression of *DAD1* was down-regulated in both these samples. The *IGF2* and *H19* genes were oppositely expressed between HBL_184 and HBL_231, having UPD within 11p15.

Discussion

The present study represents the application of the SNP array technology for the genome-wide analysis of CN aberrations in HBL. Several recent studies and our previous research have demonstrated that this technology provided a unique opportunity to assess the DNA CN alterations and LOH simultaneously throughout the entire genome.[24–27,29] As shown in the present analysis, the use of high-resolution SNP arrays improved the ability to identify structural chromosomal aberrations in cancer cells and detect genes affected by these aberrations. Additionally, high-density SNP array analysis with the CN analyzer software can also

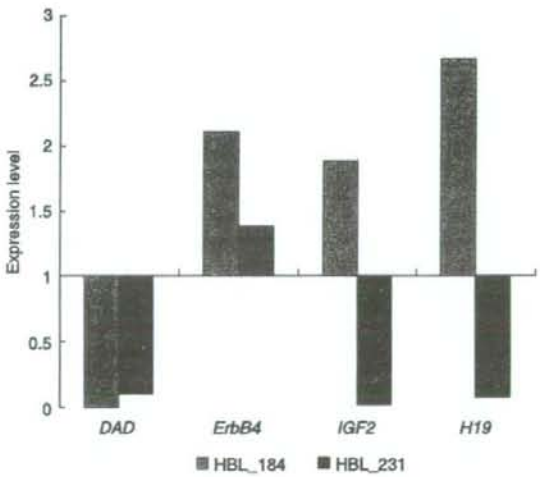

Fig. 5. The results of the expression levels of four genes (defender against cell death 1 [*DAD1*], EPH receptor B6 [*EphB6*], *ErbB4*, insulin-like growth factor II [*IGF2*], and *H19* genes) through real-time quantitative reverse transcription-polymerase chain reaction (RQ-RT-PCR) analyses.

doi: 10.1111/j.1349-7006.2007.00710.x
© 2008 Japanese Cancer Association

facilitate the identification of allelic imbalances such as copy-neutral LOH in the absence of a paired normal DNA reference.

The aberrations in chromosomes 1q, 2, 8, and 20 have been noted as the most commonly occurring aberrations in all previous reports,[21,22] as well as in the present study. In the present study, the most frequently detected aberrations were gains in chromosomes 1q and 2 (or 2q), observed in approximately 50% of the cases.

Trisomy in chromosome 1q is a well-known alteration in HBL.[34] Similar 1q imbalances have also been described in other pediatric neoplastic disorders such as lymphoma,[35] Wilms' tumor,[36] and sarcoma,[37] indicating that these aberrations are related to tumor progression. The candidate genes in 1q included the *NTRK1*, *ABL2*, *CD34*, *DAP3* (death receptor protein-3), and caspase-3 genes.[38] The anomalies in chromosome 2, which almost always result in gains in 2q, are also common in HBL. These imbalances are also commonly found in embryonal rhabdomyosarcoma and other pediatric tumors related to BWS. Translocation involving the *PAX3* gene located in 2q35 has been suggested to play a crucial role in the pathogenesis of alveolar rhabdomyosarcoma.[39] Based on this, a genetic link has been suggested between HBL and alveolar rhabdomyosarcoma. The role of the *PAX3* gene in the pathogenesis of HBL is yet to be determined. Additionally, the 2q24–32 region contains several genes that may also have an oncogenic potential. These include a serine/threonine kinase receptor, *ITRAF*, *FRZB*, a secreted antagonist of WNT signaling, and BRCA1-associated RING domain 1 (*BARD1*) genes. However, no specific gene has been identified in the previous,[21,22] and present studies.

The losses in chromosomes 4q and 11q were comprehensively observed. In hepatocellular carcinoma (HCC) cells, Wong *et al.* demonstrated a growth advantage following the loss in the 4q arm.[40] In HCC, 4q21–q22 and 4q35 have been identified as commonly deleted regions, and allelic losses in 4q35 have been associated with a larger tumor size and an aggressive histological tumor type.[41] Previous studies have not reported a significant correlation between HBL with loss in the distal 4q arm and prognosis, but the underlying oncogenic event might be due to the loss of a gene on the distal 4q arm.

Many minimal regions of amplification and deletion were detected using high-density SNP arrays, although homozygous deletion was not identified in any sample. The SNP loci located in 7q34 and 14q11.2 were found to be highly amplified in sporadic HBL samples. The candidate genes at these loci are *EphB6*, *DAD1*, and BCL-like 2 (*BCL2L2*) genes that encode the proteins associated with the execution of cell apoptosis. Gains as well as high amplifications in this region have not been reported previously; however, such an observation will be of particular interest for the discovery of oncogenes involved in the pathogenesis of HBL.

The UPD regions were identified in five of the 17 samples. This is chiefly important because UPD is being particularly considered as a possible mechanism of tumor initiation. During tumorigenesis, UPD is believed to arise due to a mitotic recombination caused by a rare crossover event during mitotic cell division. The products of mitotic recombination are the regions of the genome exhibiting UPD, and both the genomic regions originate from the same parent. We could identify a common UPD on chromosome 11p that is reminiscent of BWS with paternal UPD; in this case, the loss of function of the 11p15 maternal alleles through various mechanisms may be the critical event associated with tumorigenesis and BWS.[42] BWS is a neonatal overgrowth syndrome that predisposes an individual to cancer,[6] and the importance of the maternally active locus in chromosome 11p15 in tumorigenesis is supported by the finding that the loss of imprinted allele and paternal duplication leads to tissue overgrowth and subsequent tumor development. Methylation analysis was performed for the four HBL samples having UPD within 11p15, and hypermethylation of *H19* DMR was detected in all four HBL samples. Because *H19* DMR was hypermethylated on the paternal allele and hypomethylated on the maternally expressed allele in humans, we consider that the UPD within 11p15 was of paternal origin.

Two candidate genes, namely, *IGF2* and *H19*, are located within the telomeric region of chromosome 11p15.5 and have opposite imprinting patterns.[43] In the majority of human tissues, *IGF2* is expressed only from the paternal allele, whereas *H19* is transcribed only from the maternal allele. *H19* is an untranslated gene but has been suggested to function as a tumor suppressor.[44] In fetal and adult organs, the transcriptionally silent *H19* allele was extensively hypermethylated throughout the entire gene and its promoter. On the maternally expressed *H19* allele, *H19* DMR is unmethylated and can bind to the CTCF protein. On the paternal *H19* allele, *H19* DMR is highly methylated. This not only prevents the expression of the imprinted paternal *H19* alleles but also blocks the binding of the CTCF protein.[43] In general, the outcome of UPD with losses of the 11p15 maternal alleles in HBL is the same as that of the loss of imprinting on the inactivated, imprinted, and maternally expressed genes in BWS. Weksberg *et al.* proposed a dual pathway model for tumor development in BWS, wherein methylation defects at *H19* and/or *IGF2* in 11p15 were found to play a role in Wilms' and HBL tumorigenesis.[45] The combined loss of expressions in various 11p15-imprinted genes may contribute to tumorigenesis.

In the present study, we identified that the expression patterns of *IGF2* and *H19* were opposite between genes with and without the UPD in 11p15. This difference in the expression patterns might influence the clinical features of HBL. Further prospective studies are required to reveal any potential correlations between specific LOH and clinical outcomes.

In summary, the analysis of LOH and CN alterations using the SNP microarray in HBL samples revealed significant areas of allelic imbalance. We hypothesize that UPD, in addition to allelic imbalance, constitutes a novel genetic mechanism involved in tumorigenesis. Therefore, detailed characterizations such as functional studies should be conducted to elucidate the significance of the regions detected in this study, many of which may contain the candidate tumor suppressor genes and oncogenes involved in the pathogenesis of HBL.

Acknowledgments

This work was supported in part by a Grant-in-Aid for Cancer Research from the Ministry of Health, Labour and Welfare of Japan, a Grant-in-Aid for Scientific Research from the Ministry of Education, Culture, Sports, Science and Technology of Japan, and a grant from the 21st Century COE Program from the Ministry of Education, Culture, Sports, Science and Technology of Japan.

References

1 Roebuck DJ, Perilongo G. Hepatoblastoma: an oncological review. *Pediatr Radiol* 2006; **36**: 183–6.
2 Tiao GM, Bobey N, Allen S *et al.* The current management of hepatoblastoma: a combination of chemotherapy, conventional resection, and liver transplantation. *J Pediatr* 2005; **146**: 204–11.
3 Schnater JM, Kohler SE, Lamers WH, von Schweinitz D, Aronson DC. Where do we stand with hepatoblastoma? A review. *Cancer* 2003; **98**: 668–78.
4 Ikeda H, Matsuyama S, Tanimura M. Association between hepatoblastoma and very low birth weight: a trend or a chance? *J Pediatr* 1997; **130**: 557–60.
5 Hughes LJ, Michels VV. Risk of hepatoblastoma in familial adenomatous polyposis. *Am J Med Genet* 1992; **43**: 1023–5.
6 DeBaun MR, Tucker MA. Risk of cancer during the first four years of life in children from The Beckwith–Wiedemann Syndrome Registry. *J Pediatr* 1998; **132**: 398–400.
7 Fukuzawa R, Hata J, Hayashi Y, Ikeda H, Reeve AE. Beckwith–Wiedemann syndrome-associated hepatoblastoma: wnt signal activation occurs later in

© 2008 Japanese Cancer Association

tumorigenesis in patients with 11p15.5 uniparental disomy. *Pediatr Dev Pathol* 2003; **6**: 299–306.
8 Little MH, Thomson DB, Hayward NK, Smith PJ. Loss of alleles on the short arm of chromosome 11 in a hepatoblastoma from a child with Beckwith–Wiedemann syndrome. *Hum Genet* 1988; **79**: 186–9.
9 Albrecht S, von Schweinitz D, Waha A, Kraus JA, von Deimling A, Pietsch T. Loss of maternal alleles on chromosome arm 11p in hepatoblastoma. *Cancer Res* 1994; **54**: 5041–4.
10 Oda H, Imai Y, Nakatsuru Y, Hata J, Ishikawa T. Somatic mutations of the APC gene in sporadic hepatoblastomas. *Cancer Res* 1996; **56**: 3320–3.
11 Lengauer C, Kinzler KW, Vogelstein B. Genetic instabilities in human cancers. *Nature* 1998; **396**: 643–9.
12 Yeh YA, Rao PH, Cigna CT, Middlesworth W, Lefkowitch JH, Murty VV. Trisomy 1q, 2, and 20 in a case of hepatoblastoma: possible significance of 2q35-q37 and 1q12-q21 rearrangements. *Cancer Genet Cytogenet* 2000; **123**: 140–3.
13 Nagata T, Mugishima H, Shichino H *et al.* Karyotypic analyses of hepatoblastoma. Report of two cases and review of the literature suggesting chromosomal loci responsible for the pathogenesis of this disease. *Cancer Genet Cytogenet* 1999; **114**: 42–50.
14 Sainati L, Leszl A, Stella M *et al.* Cytogenetic analysis of hepatoblastoma: hypothesis of cytogenetic evolution in such tumors and results of a multicentric study. *Cancer Genet Cytogenet* 1998; **104**: 39–44.
15 Tonk VS, Wilson KS, Timmons CF, Schneider NR. Trisomy 2, trisomy 20, and del (17p) as sole chromosomal abnormalities in three cases of hepatoblastoma. *Genes Chromosomes Cancer* 1994; **11**: 199–202.
16 Park JP, Omvold KT, Brown AM, Mohandas TK. Trisomy 2 and 19, and tetrasomy 1q and 14 in hepatoblastoma. *Cancer Genet Cytogenet* 1999; **115**: 86–7.
17 Balogh E, Swanton S, Kiss C, Jakab ZS, Secker-Walker LM, Olah E. Fluorescence in situ hybridization reveals trisomy 2q by insertion into 9p in hepatoblastoma. *Cancer Genet Cytogenet* 1998; **102**: 148–50.
18 Sainati L, Leszl A, Surace C, Perilongo G, Rocchi M, Basso G. Fluorescence in situ hybridization improves cytogenetic results in the analysis of hepatoblastoma. *Cancer Genet Cytogenet* 2002; **134**: 18–20.
19 Surace C, Leszl A, Perilongo G, Rocchi M, Basso G, Sainati L. Fluorescent in situ hybridization (FISH) reveals frequent and recurrent numerical and structural abnormalities in hepatoblastoma with no informative karyotype. *Med Pediatr Oncol* 2002; **39**: 536–9.
20 Parada LA, Limon J, Iliszko M *et al.* Cytogenetics of hepatoblastoma: further characterization of 1q rearrangements by fluorescence in situ hybridization: an international collaborative study. *Med Pediatr Oncol* 2000; **34**: 165–70.
21 Hu J, Wills M, Baker BA, Perlman EJ. Comparative genomic hybridization analysis of hepatoblastomas. *Genes Chromosomes Cancer* 2000; **27**: 196–201.
22 Weber RG, Pietsch T, von Schweinitz D, Lichter P. Characterization of genomic alterations in hepatoblastomas. A role for gains on chromosomes 8q and 20 as predictors of poor outcome. *Am J Pathol* 2000; **157**: 571–8.
23 Janne PA, Li C, Zhao X *et al.* High-resolution single-nucleotide polymorphism array and clustering analysis of loss of heterozygosity in human lung cancer cell lines. *Oncogene* 2004; **23**: 2716–26.
24 Huang J, Wei W, Zhang J *et al.* Whole genome DNA copy number changes identified by high density oligonucleotide arrays. *Hum Genomics* 2004; **1**: 287–99.
25 Peiffer DA, Le JM, Steemers FJ *et al.* High-resolution genomic profiling of chromosomal aberrations using Infinium whole-genome genotyping. *Genome Res* 2006; **16**: 1136–48.
26 Zhao X, Li C, Paez JG *et al.* An integrated view of copy number and allelic alterations in the cancer genome using single nucleotide polymorphism arrays. *Cancer Res* 2004; **64**: 3060–71.
27 Nannya Y, Sanada M, Nakazaki K *et al.* A robust algorithm for copy number detection using high-density oligonucleotide single nucleotide polymorphism genotyping arrays. *Cancer Res* 2005; **65**: 6071–9.
28 Yamamoto G, Nannya Y, Kato M *et al.* Highly sensitive method for genomewide detection of allelic composition in nonpaired, primary tumor specimens by use of affymetrix single-nucleotide-polymorphism genotyping microarrays. *Am J Hum Genet* 2007; **81**: 114–26.
29 Wong KK, Tsang YT, Shen J *et al.* Allelic imbalance analysis by high-density single-nucleotide polymorphic allele (SNP) array with whole genome amplified DNA. *Nucleic Acids Res* 2004; **32**: e69.
30 Trask BJ. Fluorescence in situ hybridization: applications in cytogenetics and gene mapping. *Trends Genet* 1991; **7**: 149–54.
31 Herman JG, Graff JR, Myohanen S, Nelkin BD, Baylin SB. Methylation-specific PCR: a novel PCR assay for methylation status of CpG islands. *Proc Natl Acad Sci USA* 1996; **93**: 9821–6.
32 Li LC, Dahiya R. MethPrimer: designing primers for methylation PCRs. *Bioinformatics* 2002; **18**: 1427–31.
33 Koch A, Waha A, Hartmann W *et al.* Elevated expression of Wnt antagonists is a common event in hepatoblastomas. *Clin Cancer Res* 2005; **11**: 4295–304.
34 Douglass EC, Green AA, Hayes FA, Ercubanas E, Horowitz M, Wilimas JA. Chromosome 1 abnormalities: a common feature of pediatric solid tumors. *J Natl Cancer Inst* 1985; **75**: 51–4.
35 Kaneko Y, Variakojis D, Klutkens L, Rowley JD. Lymphoblastic lymphoma: cytogenetic, pathologic, and immunologic studies. *Int J Cancer* 1982; **30**: 273–9.
36 Kaneko Y, Kondo K, Rowley JD, Moohr JW, Maurer HS. Further chromosome studies on Wilms' tumor cells of patients without aniridia. *Cancer Genet Cytogenet* 1983; **10**: 191–7.
37 Nilsson M, Meza-Zepeda LA, Meriens F, Forus A, Myklebost O, Mandahl N. Amplification of chromosome 1 sequences in lipomatous tumors and other sarcomas. *Int J Cancer* 2004; **109**: 363–9.
38 Kissil JL, Kimchi A. Assignment of death associated protein 3 (DAP3) to human chromosome 1q21 by in situ hybridization. *Cytogenet Cell Genet* 1997; **77**: 252.
39 Turc-Carel C, Lizard-Nacol S, Justrabo E, Favrot M, Philip T, Tabone E. Consistent chromosomal translocation in alveolar rhabdomyosarcoma. *Cancer Genet Cytogenet* 1986; **19**: 361–2.
40 Wong N, Lai P, Lee SW *et al.* Assessment of genetic changes in hepatocellular carcinoma by comparative genomic hybridization analysis: relationship to disease stage, tumor size, and cirrhosis. *Am J Pathol* 1999; **154**: 37–43.
41 Bando K, Nagai H, Matsumoto S *et al.* Identification of a 1-cM region of common deletion on 4q35 associated with progression of hepatocellular carcinoma. *Genes Chromosomes Cancer* 1999; **25**: 284–9.
42 Koufos A, Hansen MF, Copeland NG, Jenkins NA, Lampkin BC, Cavenee WK. Loss of heterozygosity in three embryonal tumours suggests a common pathogenetic mechanism. *Nature* 1985; **316**: 330–4.
43 Hark AT, Schoenherr CJ, Katz DJ, Ingram RS, Levorse JM, Tilghman SM. CTCF mediates methylation-sensitive enhancer-blocking activity at the H19/Igf2 locus. *Nature* 2000; **405**: 486–9.
44 Zhang Y, Shields T, Crenshaw T, Hao Y, Moulton T, Tycko B. Imprinting of human H19: allele-specific CpG methylation, loss of the active allele in Wilms tumor, and potential for somatic allele switching. *Am J Hum Genet* 1993; **53**: 113–24.
45 Weksberg R, Nishikawa J, Caluseriu O *et al.* Tumor development in the Beckwith–Wiedemann syndrome is associated with a variety of constitutional molecular 11p15 alterations including imprinting defects of KCNQ1OT1. *Hum Mol Genet* 2001; **10**: 2989–3000.

doi: 10.1111/j.1349-7006.2007.00710.x
© 2008 Japanese Cancer Association

Significance of the complete clearance of peripheral blasts after 7 days of prednisolone treatment in children with acute lymphoblastic leukemia: the Tokyo Children's Cancer Study Group Study L99-15

Atsushi Manabe,[1] Akira Ohara,[2] Daisuke Hasegawa,[1] Katsuyoshi Koh,[3] Tomohiro Saito,[4] Nobutaka Kiyokawa,[5] Akira Kikuchi,[6] Hiroyuki Takahashi,[7] Koichiro Ikuta,[8] Yasuhide Hayashi,[9] Ryoji Hanada[6] and Masahiro Tsuchida[10]

[1]Tokyo Children's Cancer Study Group; Department of Pediatrics, St. Luke's International Hospital, Tokyo; [2]First Department of Pediatrics, Toho University, Tokyo; [3]Department of Pediatrics, University of Tokyo, Tokyo; [4]Departments of Health Policy and [5]Developmental Biology, National Research Institute for Child Health and Development, Tokyo; [6]Department of Hematology-Oncology, Saitama Children's Medical Center, Iwatsuki; [7]Department of Pediatrics, Saiseikai Yokohama City Nanbu Hospital, Yokohama; [8]Department of Pediatrics, Yokohama City University, School of Medicine, Yokohama; [9]Department of Hematology-Oncology, Gunma Children's Medical Center, Shibukawa and [10]Department of Pediatrics, Ibaraki Children's Hospital, Mito, Japan

Acknowledgments: we thank the members of the ALL Committee of the TCCSG: Keiichi Isoyama, Akitoshi Kinoshita, Takehiko Kamijo, Masa-aki Kumagai, Hiromasa Yabe, Tsuyoshi Morimoto, Miho Maeda, Ken-ichi Sugita, Yasushi Noguchi, Takashi Kaneko, Kanji Sugita, Manabu Sotomatsu, Michiko Kajiwara, Yuri Okimoto, Setsuo Ohta, Masahiro Saito, and Takashi Fukushima. We also thank Kaori Itagaki for preparing and refining the patients' data and Dr. Kazuko Kudo for valuable discussion. Finally, we thank all the pediatricians and nurses.

Manuscript received October 10, 2007. Revised version arrived on March 3, 2008. Manuscript accepted April 2, 2008.

Correspondence:
Atsushi Manabe, MD, PhD,
Department of Pediatrics,
St. Luke's International Hospital, 9-1,
Akashi-cho, Chuo-ku,
Tokyo 104-8560, Japan.
E-mail: manabe-luke@umin.ac.jp

ABSTRACT

Background

Treatment response has become one of the most important prognostic factors in childhood acute lymphoblastic leukemia. We evaluated the significance of the complete clearance of peripheral leukemic blasts on survival in children with acute lymphoblastic leukemia.

Design and Methods

Seven hundred and fifty-four children diagnosed with acute lymphoblastic leukemia, consecutively enrolled from 1999 to 2003 in the TCCSG L99-15 study, were eligible for analysis. Patients were stratified into three risk groups based on presenting features, such as age and the leukocyte count before starting the treatment, followed by reclassification into three categories 7 days after prednisolone monotherapy based on the peripheral blast count; 0/μL (*Day8NoBlasts*), 1-999/μL and ≥ 1,000/μL.

Results

After 7 days of prednisolone monotherapy, 249 patients (33%) were classified as *Day8NoBlasts*, 392 patients (52%) had blast counts of 1-999/μL, and 113 patients (15%) had blast counts ≥ 1,000/μL. The event-free survival for all patients was 79.6±1.6 (SE)% at 4 years, whereas that for patients with *Day8NoBlasts* was 90.4±2.0% (n=249) and the event-free survival for the other patients was 74.2±2.2% (n=504) (log rank $p<0.001$). The event-free survival for *Day8NoBlasts* patients with B-lineage acute lymphoblastic leukemia and T-cell acute lymphoblastic leukemia was 89.8±2.1% (n=226) and 95.7±4.3% (n=23), respectively. In a multivariate analysis, age at diagnosis, the initial white blood cell count, immunophenotype, and gender did not remain as independent risk factors for treatment failure, whereas *Day8NoBlasts* and marked hyperdiploidy (more than 50 chromosomes) became statistically significant.

Conclusions

Children with *Day8NoBlasts* constituted one third of all the cases with childhood acute lymphoblastic leukemia with an excellent outcome, and should be candidates for curative management with less intensive treatment.

Key words: lymphoblastic leukemia, children, clearance of blasts, steroid response.

Citation: Manabe A, Ohara A, Hasegawa D, Koh K, Saito T, Kiyokawa N, Kikuchi A, Takahashi H, Ikuta K, Hayashi Y, Hanada R, and Tsuchida M. Significance of the complete clearance of peripheral blasts after 7 days of prednisolone treatment in children with acute lymphoblastic leukemia: the Tokyo Children's Cancer Study Group Study L99-15. Haematologica 2008; 93:1155-1160. doi: 10.3324/haematol.12365

©2008 Ferrata Storti Foundation. This is an open-access paper.

©Ferrata Storti Foundation

Introduction

Early treatment response is one of the most useful prognostic indicators in childhood acute lymphoblastic leukemia (ALL). This response depends on numerous variables, including the clinicobiological features of the disease, chemotherapy dosages, and also the ability of individual patients to metabolize antileukemic drugs.[1,2] The level of circulating lymphoblasts after 1 week of chemotherapy is associated with the risk of relapse.[3-7] The Berlin-Franfurt-Münster (BFM) group has traditionally employed the response to prednisolone for 7 days and one dose of intrathecal methotrexate to stratify patients: a cut-off peripheral blood blast count of 1,000/μL is used to assign patients into two groups; that is, prednisolone good responders and prednisolone poor responders.[3,8] The utility of this method has been well appreciated and is now employed by other study groups.[9-11]

We analyzed the results of the L89-12 study of the Tokyo Children's Cancer Study Group (TCCSG), and found that a cut-off of 1,000 blasts/μL after a 7-day course of prednisolone monotherapy was useful for stratifying patients.[12] We also found that patients without detectable blasts in the peripheral blood had an even better prognosis (*unpublished data*). In the 99-15 study, we employed a cut-off of 0 blasts in addition to 1,000 blasts to stratify children with ALL. Here, we report the treatment outcome of the study, in which the utility of the above-mentioned stratification of the patients was examined.

Design and Methods

Patients

Seven hundred and seventy children (1 to 18 years of age) diagnosed with ALL were consecutively enrolled from February 1999 to July 2003 in the TCCSG L99-15 study. Children less than 1 year of age were excluded from this study and treated with an infant ALL protocol. Sixteen patients were not evaluable; therefore, 754 patients (male: female; 428:326) were eligible for analysis. Their median age was 5 years (range, 1-17). Written informed consent was obtained from parents or guardians and from the patients as appropriate for their age and conceptual ability.

The diagnosis of ALL was based on morphological, biochemical, and flow cytometric features of leukemic cells, including lymphoblast morphology on May- or Wright-Giemsa-stained bone marrow smears, negative staining for myeloperoxidase, and reactivity with monoclonal antibodies to B- or T-lineage-associated lymphoid differentiation antigens. Remission was defined as the presence of fewer than 5% blasts with the recovery of hematopoiesis.

Day 8 risk classification

The patients were stratified into three risk groups based on presenting features (age and the leukocyte count before starting the treatment) and then reclassified into three categories 7 days later according to the sensitivity to oral prednisolone monotherapy, the dose of which was 30-60 mg/m²/day (Table 1). A total dose of at least 210 mg/m² of prednisolone was to be administered in this 7-day prephase period. A diagnostic lumbar puncture was performed and initial intrathecal methotrexate was given on day 8.[12] The dividing counts of 0 blasts/μL and 1,000 blasts/μL were used to stratify patients. To count blasts in the peripheral blood, 200 cells were morphologically assessed under a microscope.

Day 43 risk classification

The patients were finally stratified based on the bone marrow status examined between 43 and 50 days after the initiation of remission induction therapy and on cytogenetic findings. Patients who did not achieve remission and those with the Philadelphia chromosome or 11q23 rearrangements were allocated to the high risk group and underwent allogeneic stem cell transplantation, and those initially at standard risk who showed t(1;19) were switched into the intermediate risk group. The median follow-up period of patients was 3.8 years.

Treatment protocol

The protocol was approved by the institutional review boards of the participating institutions or the equivalent organization. Treatment regimens are detailed in Table 2. A proportion of patients in the high risk group underwent stem cell transplantation in first

Table 1. Risk stratification.

		B-lineage ALL	
Initial risk WBC (×10⁹/L)	1-6 years	7-9 years	>10 years
<20	SR	IR	IR
20-50	IR	IR	IR
50-100	IR	IR	HR
≥100×10⁹/L	HR	HR	HR
		Day 8 risk (final risk)	
Day 8 PB Blasts	0	1-999	≥1,000/μL
Day 1 SR	SR	SR	IR
Day 1 IR	IR	IR	HR
Day 1 HR	IR	HR	Allo-SCT
		T-ALL	
Day 8 PB blasts	0	1-999	≥1,000/μL
All patients*	IR	HR	Allo-SCT

*WBC: white blood cell count; PB: peripheral blood; SR: standard risk; IR: intermediate risk; HR: high risk; allo-SCT: allogeneic stem cell transplantation; *in T-ALL, patients were stratified only based on the day 8 PB blast count regardless of age and initial WBC. Patients with ALL, from 1 to 18 years of age at diagnosis. Philadelphia chromosome and MLL rearrangement: Allo-SCT, t(1;19): Shifted to IR from SR. Cranial irradiation: patients with initial WBC > 100×10⁹/L: 12 Gy for those aged 1-6 years, 18 Gy for the others.*

©Ferrata Storti Foundation

remission according to the protocol (n=58). Prophylactic cranial irradiation was given only to patients with an initial leukocyte count exceeding 100×10^9/L. The dose of irradiation was 12 Gy for patients aged between 1 and 6, and 18 Gy for the others. A maintenance phase, consisting of 6-mercaptopurine and methotrexate, was continued until week 146 in the standard risk group and until week 104 in the intermediate risk group, whereas no maintenance therapy was given to patients in the high risk group.

Two randomizations were performed. The first randomization concerned the schedule of L-asparaginase in the remission induction phase in the standard and intermediate risk groups: two doses a week *vs.* three doses a week for a total number of nine doses in both groups. The second randomization involved only intermediate risk patients: high-dose cytarabine at 2 g/m² 8 times *vs.* cytarabine at 75 mg/m² 15 times accompanied by cyclophosphamide at 1,000 mg/m² and 6-mercaptopurine at 60 mg/m² 21 times in the post-remission induction intensification phase. No differences in event-free survival had been documented previously;[15] we, therefore, analyzed the randomized patients as a single subset. The detailed results of these randomizations will be reported separately.

Table 2. Treatment regimens.

Standard risk
Induction: Pred 60 mg/m²×5 weeks, VCR 1.5mg/m² x 5, Piranubicin 20mg/m²×2, L-asp 6,000U/m²×9 (2 times/week *vs.* 3 times/week, randomized)
Intensification 1: CY 1,000 mg/m², Ara-C 75 mg/m²×15, 6MP 60mg/m²×21
Intensification 2: MTX 3 g/m²×3
Interim maintenance: 6 MP 60 mg/m²×14, MTX 25 mg/m²×3
Reinduction: Pred 60 mg/m²×14, VCR 1.5 mg/m²×3, Piranubicin 20 mg/m²×3, L-asp 10,000U/m²×4
Late intensification 1: CY 1,000 mg/m², Ara-C 75 mg/mm²×10, 6MP 60 mg/m²× 14
Late intensification 2 (3 cycles): MTX 500 mg/m², PSL/VCR/L-asp (2 wks)
Maintenance: 6 MP/MTX until week 146.
Total number of IT therapies: 11

Intermediate risk
Induction: Pred 60 mg/m²×5 wks, VCR 1.5 mg/m²×5, DNR 25 mg/m²×4, CY 1,000 mg/m²×2, L-asp 6000U/m²×9 (2 times a week *vs.* 3 times a week)
Intensification 1 (Randomized): High-dose Ara-C (2 g/m²×8), L-asp (10,000U/m²) *vs.* CY 1,000 mg/m², Ara-C 75 mg/m²×15, 6 MP 60 mg/m²×21
Intensification 2: MTX 3 g/m²×3
Interim maintenance: 6 MP 60 mg/m²×14, MTX 25 mg/m²×3
Reinduction 1: DEXA 6 mg/m²×14, VCR 1.5 mg/m²×4, DXR 25 mg/m²×4, L-asp 10,000U/m²×4
Late intensification 1: CY 1,000 mg/m², Ara-C 75mg/m²×10, 6MP 60 mg/m²× 14
Late intensification 2 (2 cycles): Ara-C 2 g/m²×4 with L-asp 10,000U/m²×1, MTX 500 mg/m²
Reinduction 2: Pred 60 mg/m²×14, VCR 1.5 mg/m²×3, Piranubicin 20 mg/m²× 3
L-asp 10,000 U/m² × 4
Late intensification 3: CY 1,000 mg/m², Ara-C 75 mg/m² x 10, 6MP 60 mg/m² x 14
Maintenance: 6MP/MTX until week 104.
Total number of IT therapies: 10 or 11

High risk
Induction: Pred 60 mg/m²×5 weeks, VCR 1.5mg/m²×5, DNR 25 mg/m²×4, CY 1,000 mg/m²×2, L-asp 6,000U/m²×9
Intensification 1: High-dose Ara-C (2 g/m²×8) with L-asp (10,000 U/m²) CY 1,000 mg/m², Ara-C 75mg/m²×15, 6MP 60 mg/m²×21
Intensification 2 (2 cycles): Ara-C 3 g/m²×6, Etoposide 100mg/m²×5, Mitoxantrone 10 mg/m²
Allogeneic SCT if indicated. If not, proceed to the followings:
Intensification 3: high-dose MTX 3 g/m², CY 200 mg/m²×5, VCR 1.5 mg/m²
Repeat Intensification 2 twice, then repeat Intensification 3
Intensification 4 (2 cycles): Ara-C 3 g/m²×4, L-asp 10,000 U/m²
Cranial irradiation with 6MP 60 mg/m²×14
No maintenance: Treatment stopped at week 48
Total number of IT therapies: 9-17

Statistical analysis

The duration of event-free survival was defined as the time from the initiation of therapy to either treatment failure (relapse, death, or diagnosis of secondary cancer) or to the last day when the patient was confirmed to be in remission. In those patients who did not achieve complete remission after the first induction phase or who died before the confirmation of remission, treatment was considered to have failed at day 0. The probability of event-free survival was estimated by the Kaplan-Meier method, and was tested for significance using the log-rank test.

For multivariate analysis, the Cox proportional hazards model was employed to assess independent effects of risk factors on event-free survival. All calculations were performed by PC-SAS (SAS Institute Inc., PC-SAS, version 8, 2000, Cary, NC, USA).

Results

The numbers of peripheral leukemic blasts on day 8

The number of leukemic blasts was assessed in all patients (Table 3). Prephase prednisolone was administered to all the patients except six in whom vincristine and/or cyclophosphamide was used before day 8 because of insufficient cytoreduction. Overall, blasts were not detectable in 249 patients (33.0%) (*Day8NoBlasts*), 392 patients (52.0%) had a blast count of 1-999/μL, and 113 patients (15.0%) had a blast count ≥ 1,000/μL. In the subset of 90 patients with T-ALL, 23 (25.6%) fell in the *Day8NoBlasts* group, whereas 226 (34.0%) out of the 664 patients with B-lineage ALL belonged to the *Day8NoBlasts* group. Of note, 15

Table 3. The number of patients stratified by peripheral blood leukemic blast count on day 8.

Immunophenotype	*The number of peripheral blood leukemic blasts per μL*		
	0	*1-999*	*≥1,000*
B-lineage ALL			
Initial SR group	132*	148	22
Initial IR group	88	175	34
Initial HR group	6	34	25
T-ALL	23	35	32

*SR: standard risk; IR: intermediate risk; HR: high risk. *The numbers of patients in each category are shown.*

©Ferrata Storti Foundation

patients (9 with T-ALL and 6 with B-lineage ALL) in the initial high risk group achieved the status of *Day8NoBlasts*, despite high initial leukocyte counts exceeding 50,000/μL.

Subsets of patients with abnormal karyotypes were further analyzed: 25 (35.7%) of the 70 patients with *TEL/AML1* rearrangement achieved *Day8NoBlasts*, as did 69 (37.9%) of the 182 patients with high hyperdiploidy (more than 50 chromosomes), 3 (8.1%) of the 37 patients with *E2A/PBX1* rearrangement, 4 (36%) of the 11 patients with *MLL* rearrangement, and 2 (11.8%) of the 17 patients with the *BCR/ABL* fusion.

Treatment outcome

Remission was achieved in 736 (97.6%) of the 754 patients: non-T ALL: 98.6%, T-ALL: 94.4%. The probability of event-free survival for all patients was 79.6±1.6% (SE) % at 4 years, whereas the event-free survival rates for patients with B-lineage ALL and T-ALL were 80.5±1.7% (n=664) and 66.0±5.1% (n=90), respectively (Figure 1). The event-free survival for patients stratified finally on day 43 (T-cell ALL included) were as follows: 92.4±1.8% in the standard risk group (n=262), 80.3±2.6% in the intermediate risk group (n=313), and 57.8±4.1% in the high risk group (n=179). The event-free survival for patients with *Day8NoBlasts* was 90.4±2.0% (n=249), which was significantly better than that for the other patients (74.2±2.2%; $p<0.01$) (Figure 2). The event-free survival for *Day8NoBlasts* patients with T-ALL (n=23) was 95.7±4.3%, which was comparable with that of patients with B-lineage ALL (n=226), 89.8±2.1% ($p=0.45$. Figure 3).Treatment failed in only one patient with T-ALL with *Day8NoBlasts* because of death due to pancreatitis during remission induction. The event-free survival for patients with *Day8NoBlasts* and blast counts of 1-999/μL in the initial standard risk group with B-lineage ALL did not differ (90.5±2.6% *vs.* 92.5±2.5%; $p=0.82$), whereas there was a significant difference in the initial intermediate risk group with B-lineage ALL (89.4±3.6% *vs.* 72.7±3.9%; $p=0.004$). Lastly, in the initial high risk group with B-lineage ALL, five out of six patients with *Day8NoBlasts* had a good outcome.

Multivariate analysis

The significance of *Day8NoBlasts* was further analyzed using a Cox proportional hazards model. The results of the multivariate analysis are shown in Table 4. Age at diagnosis, the initial white blood cell count, immunophenotype (T-ALL *vs.* non T-ALL), and gender did not remain as statistically significant independent factors. Only *Day8NoBlasts* and high hyperdiploidy were statistically significant. We also assessed the prognostic value of *Day8NoBlasts* by dividing the counts into three categories; 0/μL, 1-999/μL, and ≥1000/μL. No difference was observed between the 1-999/μL and ≥1000/μL categories in the univariate analysis; the risk ratio for ≥1000/μL against 1-999/μL was 1.23 (95% CI: 0.98-1.56) whereas the risk ratio for ≥1000/μL against 0/μL was 0.46 (95% CI: 0.33-0.62). The results were similar when this prognostic factor was used as a three-category term in the multivariate analysis. These results led to the use of this prognostic factor as a two-category factor for simplicity and convenience for use in other studies.

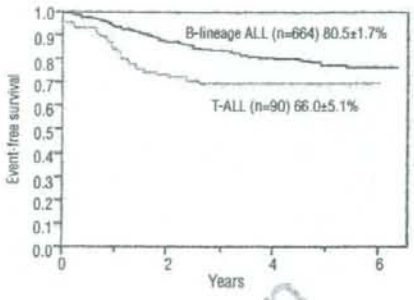

Figure 1. Kaplan-Meier plots of event-free survival according to immunophenotype (B-lineage ALL and T-ALL).

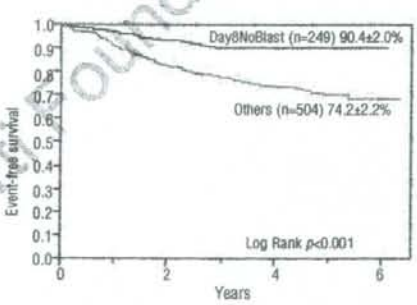

Figure 2. Kaplan-Meier plots of event-free survival of patients with no detectable blasts on day 8 and the other patients: the difference between the two curves at 4 years was highly significant ($p<0.001$ by the log-rank test).

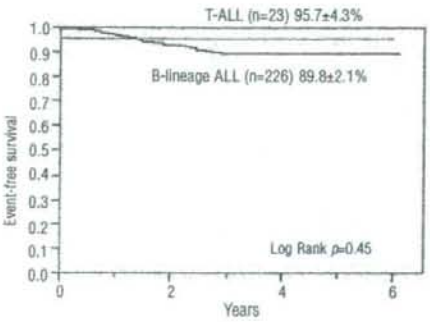

Figure 3. Kaplan-Meier plots of event-free survival of patients with no detectable blasts on day 8 divided according to the immunophenotype: the event-free survival at 4 years for *Day8NoBlasts* patients with T-ALL was comparable to that of patients with B-lineage ALL ($p=0.45$ by the log-rank test).

©Ferrata Storti Foundation

Discussion

The concept that an early response to treatment is strongly predictive of relapse has been overwhelmingly emphasized. Here, we added novel information that patients whose peripheral blood blasts disappeared after 7 days of prednisolone monotherapy had an excellent prognosis, that is, a 4-year event-free survival of 90%. Of note, such patients constituted one third of all children with ALL, thus being quite a large group. *Day8NoBlasts* was also an independent prognostic factor when assessed by multivariate analysis. Of interest, a substantial proportion of patients with *TEL/AML1* rearrangement and high hyperdiploidy achieved *Day8NoBlasts* (36% and 38%, respectively), while a very small proportion (6%) of patients with *E2A/PBX1* did so, suggesting that the kinetics of reduction in leukemic blasts may be different in subsets of patients defined by genetic changes.

One of the limitations of our study was that the enumeration of blasts in the peripheral blood was done by microscopic evaluation, which is a subjective method. The results might, therefore, not be reproducible with confidence; however, the percentages of patients with blast counts of 0/μL, 1-999/μL and ≥ 1000/μL on day 8 in the present L99-15 study (33%, 52%, 15%, respectively) were almost identical to those of our most recent L99-1502 study (31%, 53%, 16%, respectively). On the other hand, there remains a possibility that patients having been staged down by this stratification system to less intensive treatment could even have fared better (i.e. over 90%) if treated according to the older stratification system. In the next study, we plan to employ more objective methods, such as flow cytometry.[14]

In this study, we confirmed the importance of the sensitivity of leukemic blasts to steroids. Since we did not administer intrathecal therapy until day 8, our assessment of the reduction of leukemic cells in peripheral blood on day 8 should exclusively reflect an early response of leukemic blasts to steroids.[12] Steroids function as antileukemic agents mostly by inducing ALL cells to undergo apoptosis, but little was known about critical molecules involving steroid-induced apoptosis of leukemic cells. Many investigators have addressed this issue by using gene expression profiling and several candidate genes, which might be able to predict steroid sensitivity, have been identified:[15-18] apoptotic pathway-associated genes (*MCL-1, DAPK1, CASP8A2, TXNIP, ZBTB16*), carbohydrate metabolism-associated genes, MAPK pathway-associated genes, and NF-κB-associated genes. Of these genes, *CASP8A2*, a caspase 8-related molecule, was identified as a crucial molecule differentially expressed by leukemic cells at diagnosis between patients who had high and low levels of minimal residual disease in bone marrow 18 and 45 days after the initiation of induction therapy, and it can predict both *in vitro* cell growth and prognosis.[14] One could identify the new molecule, which determines steroid sensitivity, using a similar methodology, for example, comparing gene expression patterns of leukemic cells from patients with *Day8NoBlasts* with those of patients with a classic poor response to steroid.

Table 4. The results of the multivariate analysis.

Factor	Risk ratio	95% CI	p value
No blasts 0 at day 8	0.46	0.33-0.62	<0.001
High hyperdiploidy	0.66	0.51-0.84	<0.001
TEL-AML1	0.85	0.61-1.13	0.27
T-ALL	0.89	0.71-1.13	0.34
Male	0.97	0.82-1.16	0.75
Age at presentation >10 years old	1.00	0.82-1.25	0.96

The early response to steroids has been utilized to stratify children with ALL as a tradition by the BFM group since the early 1980s.[8,9] This group uses the cut-off of 1,000 blasts/μL, among other cut-offs, to identify the approximately 10% of patients with a very high risk of relapse;[19] however, the cut-off of 0 blasts has never been used.[20] We demonstrated that one-third of patients with a better prognosis could be identified by the use of this new cut-off of 0 blasts/μL. In this study, patients with no blasts on day 8 were identified not only in the initial low risk group but also in the initial higher risk groups: 94 of 362 patients with B-lineage ALL in the intermediate and high risk groups and 23 of 90 patients with T-ALL. Generally, children with T-ALL have a poorer outcome than those with B-lineage ALL and need more intensive treatment. We, however, showed that patients with T-ALL as well as those with B-lineage ALL had a favorable outcome if circulating leukemia cells could not be detected on day 8 of therapy. By using the cut-off of 0 blasts, we could select patients, including those with B-lineage ALL in the initial higher risk groups and those with T-ALL, who could be targeted for treatment reduction, as some previous studies showed that a subset of patients with ALL could be cured with less intensive regimens.[21,22]

Authorship and Disclosures

AM and AO designed the research, analyzed data and wrote the paper; DH analyzed the data and reconstructed the text; KI, RH and MT designed the research; AO, KK, TS, NK, AK, HT and YH analyzed the data; MT is a chairman of the TCCSG.

The authors reported no potential conflicts of interest.

©Ferrata Storti Foundation

References

1. Pui CH, Campana D, Evans WE. Childhood acute lymphoblastic leukemia: current status and future perspectives. Lancet Oncol 2001;2: 597-607.
2. Pui CH, Relling MV, Downing JR. Acute lymphoblastic leukemia. N Engl J Med 2004;350:1535-48.
3. Riehm H, Reiter A, Schrappe M, Berthold F, Dopfer R, Gerein V, et al. Corticosteroid-dependent reduction of leukocyte count in blood as a prognostic factor in acute lymphoblastic leukemia in childhood (therapy study ALL-BFM 83). Klin Paediatr 1987;199:151-60.
4. Gajjar A, Ribeiro R, Hancock ML, Rivera GK, Mahmoud H, Sandlund JT, et al. Persistence of circulating blasts after 1 week of multiagent chemotherapy confers a poor prognosis in childhood acute lymphoblastic leukemia. Blood 1995;86: 1292-5.
5. Lilleyman JS, Gibson BE, Stevens RF, Will AM, Hann IM, Richards SM, et al. Clearance of marrow infiltration after 1 week of therapy for childhood lymphoblastic leukaemia: clinical importance and the effect of daunorubicin: the Medical Research Council's Working Party on Childhood Leukaemia. Br J Haematol 1997;97:603-6.
6. Schrappe M, Arico M, Harbott J, Biondi A, Zimmermann M, Conter V, et al. Philadelphia chromosome-positive (Ph^+) childhood acute lymphoblastic leukemia: good initial steroid response allows early prediction of a favorable treatment outcome. Blood 1998;92:2730-41.
7. Dordelmann M, Reiter A, Borkhardt A, Ludwig WD, Gotz N, Viehmann S, et al. Prednisone response is the strongest predictor of treatment outcome in infant acute lymphoblastic leukemia. Blood 1999;94:1209-17.
8. Reiter A, M Schrappe, Ludwig WD, Hiddemann W, Sauter S, Henze G, et al. Chemotherapy in 998 unselected childhood acute lymphoblastic leukemia patients. Results and conclusions of the multicenter trial ALL-BFM 86. Blood 1994;84:3122-33.
9. Duval M, Suciu S, Ferster A, Rialland X, Nelken B, Benoit Y, et al. Comparison of Escherichia coli-asparaginase with Erwinia-asparaginase in the treatment of childhood lymphoid malignancies: results of a randomized European Organisation for Research and Treatment of Cancer-Children's Leukemia Group phase 3 trial. Blood 2002;99:2734-9.
10. Arico M, Valsecchi MG, Conter V, Rizzari C, Pession A, Messina C, et al. Improved outcome in high-risk childhood acute lymphoblastic leukemia defined by prednisone-poor response treated with double Berlin-Frankfurt-Münster protocol II. Blood 2002;100:420-6.
11. Kamps WA, Bokkerink JP, Hakvoort-Cammel FG, Veerman AJ, Weening RS, van Wering ER, et al. BFM-oriented treatment for children with acute lymphoblastic leukemia without cranial irradiation and treatment reduction for standard risk patients: results of DCLSG protocol ALL-8 (1991-1996). Leukemia 2002;16:1099-111.
12. Manabe A, Tsuchida M, Hanada R, Ikuta K, Toyoda Y, Okimoto Y, et al. Delay of the diagnostic lumbar puncture and intrathecal chemotherapy in children with acute lymphoblastic leukemia who undergo routine corticosteroid testing: Tokyo Children's Cancer Study Group study L89-12. J Clin Oncol 2001;19: 3182-7.
13. Manabe A, Ohara A, Ikuta K, Hanada R, Yabe H, Kinoshita A, et al. The effect of early high dose Ara-C in children with high-risk acute lymphoblastic leukemia (ALL): Tokyo Children's Cancer Study Group (TCCSG) study L99-15. Blood 2005; 106:255a. [abstract]
14. Borowitz MJ, Devidas M, Bowman WP, Carroll WL, Chen IM, Harvey R, et al. Prognostic significance of minimal residual disease (MRD) in childhood B-precursor ALL and its relation to other risk factors. A Children's Oncology Group (COG) study. Blood 2006;108:69a[abstract].
15. Holleman A, Cheok MH, den Boer ML, Yang W, Veerman AJ, Kazemier KM, et al. Gene-expression patterns in drug-resistant acute lymphoblastic leukemia cells and response to treatment. N Engl J Med 2004;351:533-42.
16. Flotho C, Coustan-Smith E, Pei D, Iwamoto S, Song G, Cheng C, et al. Genes contributing to minimal residual disease in childhood acute lymphoblastic leukemia: prognostic significance of CASP8AP2. Blood 2006; 108:1050-7.
17. Tissing WJ, den Boer ML, Meijerink JP, Menezes RX, Swagemakers S, van der Spek PJ, et al. Genomewide identification of prednisolone-responsive genes in acute lymphoblastic leukemia cells. Blood 2007;109:3929-35.
18. Holleman A, den Boer ML, de Menezes RX, Cheok MH, Cheng C, Kazemier KM, et al. The expression of 70 apoptosis genes in relation to lineage, genetic subtype, cellular drug resistance, and outcome in childhood acute lymphoblastic leukemia. Blood 2006;107:769-76.
19. Schrappe M, Reiter A, Zimmermann M, Harbott J, Ludwig WD, Henze G, et al. Long-term results of four consecutive trials in childhood ALL performed by the ALL-BFM study group from 1981 to 1995. Berlin-Frankfurt-Münster. Leukemia 2000; 14:2205-22.
20. Lauten M, Stanulla M, Zimmermann M, Welte K, Riehm H, Schrappe M. Clinical outcome of patients with childhood acute lymphoblastic leukaemia and an initial leukaemic blood blast count of less than 1000 per microliter. Klin Padiatr 2001;213: 169-74.
21. Toyoda Y, Manabe A, Tsuchida M, Hanada R, Ikuta K, Okimoto Y, et al. Six months of maintenance chemotherapy after intensified treatment for acute lymphoblastic leukemia of childhood. J Clin Oncol 2000;18:1508-16.
22. Pui CH, Aur RJ, Bowman WP, Dahl GV, Dodge RK, George SL, et al. Failure of late intensification therapy to improve a poor result in childhood lymphoblastic leukemia. Cancer Res 1984;44:3593-8.

©Ferrata Storti Foundation

Supplemental Material can be found at:
http://www.jbc.org/cgi/content/full/M802315200/DC1

THE JOURNAL OF BIOLOGICAL CHEMISTRY VOL. 283, NO. 39, pp. 26820–26828, September 26, 2008
© 2008 by The American Society for Biochemistry and Molecular Biology, Inc. Printed in the U.S.A.

Fusion of OTT to BSAC Results in Aberrant Up-regulation of Transcriptional Activity*[S]

Received for publication, March 25, 2008, and in revised form, July 21, 2008 Published, JBC Papers in Press, July 30, 2008 DOI 10.1074/jbc.M802315200

Taisuke Sawada[‡], Chiharu Nishiyama[§], Takuma Kishi[‡], Tomonari Sasazuki[‡], Sachiko Komazawa-Sakon[‡], Xin Xue[‡], Jiang-Hu Piao[‡¶‖], Hideko Ogata[‡], Jun-ichi Nakayama[**], Tomohiko Taki[‡‡], Yasuhide Hayashi[§§], Mamoru Watanabe[¶¶], Hideo Yagita[‡], Ko Okumura[‡], and Hiroyasu Nakano[‡1]

From the [‡]Department of Immunology, [§]Atopy (Allergy) Research Center, and [¶]Sportology Center, Juntendo University School of Medicine, 2-1-1 Hongo, Bunkyo-ku, Tokyo 113-8421, Japan, the [‖]Department of Immunology, School of Basic Medical Science, Ningxia Medical College, Xingqing-Qu, Yinchuan 750004, China, the [**]Laboratory for Chromatin Dynamics, Center for Developmental Biology, RIKEN, 2-2-3 Minatojima-Minamimachi, Chuo-ku, Kobe 650-0047, Japan, the [‡‡]Department of Molecular Laboratory Medicine, Kyoto Prefectural University of Medicine Graduate School of Medical Science, 465 Kajii-cho kawaramachi-Hirokoji, Kamigyo-ku, Kyoto 602-8566, Japan, the [§§]Gunma Children's Medical Center, 779 Shimohakoda, Kitatachibana, Gunma 377-8577, Japan, and the [¶¶]Department of Gastroenterology and Hepatology, Tokyo Medical and Dental University, 1-5-45 Yushima, Bunkyo-ku, Tokyo 113-8519, Japan

***OTT/RBM15-BSAC/MAL/MKL1/MRTF-A* was identified as a fusion transcript generated by t(1;22)(p13;q13) in acute megakaryoblastic leukemia. Previous studies have shown that BSAC (basic, SAP, and coiled-coil domain) activates the promoters containing CArG boxes via interaction with serum response factor, and OTT (one twenty-two) negatively regulates the development of megakaryocytes and myeloid cells. However, the mechanism by which OTT-BSAC promotes leukemia is largely unknown. Here we show that OTT-BSAC, but not BSAC or OTT strongly activates several promoters containing a transcription factor Yin Yang 1-binding sequence. In addition, although BSAC predominantly localizes in the cytoplasm and its nuclear translocation is considered to be regulated by the Rho-actin signaling pathway, OTT-BSAC exclusively localizes in the nucleus. Moreover, OTT interacts with histone deacetylase 3, but this interaction is abolished in OTT-BSAC. Collectively, these functional and spatial changes of OTT and BSAC caused by the fusion might perturb their functions, culminating in the development of acute megakaryoblastic leukemia.**

Transcriptional activation of many genes depends on activities of the transcriptional factors that recognize specific target sequences but also the chromatin structures. Histone acetyltransferases and histone deacetylases (HDACs)[2] are recruited to target genes through association with specific transcriptional factors (1, 2). Histone acetyltransferases relax chromatin structures and activate transcription by acetylating histones, whereas HDACs condense chromatin structures and repress transcription by deacetylating histones (1, 2). So far, there have been three HDAC families identified (3). Class I HDACs (HDAC1, -2, -3, and -8) are closely related to the yeast transcriptional regulator RPD3 and expressed in most cell types. Class II HDACs (HDAC4, -5, -6, -7, -9, and -10) share domains with a similarity to HDA1, another deacetylase in yeast. Class III HDACs are related to the yeast silencing protein SIR2 and are dependent on NAD for enzymatic activity. HDACs exist in cells as a part of large molecular weight complex containing adaptor molecules, including Sin3A, SMRT (silencing mediator for retinoid and thyroid receptors), N-CoR (nuclear receptor corepressor), and/or SHARP (SMRT and HDAC1-associated repressor protein) (4). SHARP belongs to a family of RNA recognition motif proteins and also has a SMRT-interacting domain at the C terminus, which mediates the interaction with SMRT, N-CoR, and HDACs (5). The SMRT-interacting domain is also characterized as a SPOC (spen paralog and ortholog C-terminal) domain that was found in *Drosophila* spen and spen-like protein (6).

The t(1;22)(p13;q13) is exclusively associated with infant acute megakaryoblastic leukemia. Two groups have been independently identified as a fusion transcript that is generated by this chromosomal translocation and composed of two novel genes, designated OTT (one twenty-two) or RNA-binding motif protein (RBM) 15 and megakaryocytic acute leukemia (MAL) or megakaryoblastic leukemia-1(MKL1) (7, 8). OTT contains three RNA recognition motifs and SPOC domain (7, 8), whereas MAL is composed of N-terminal basic, glutamine-

* This work was supported in part by a Grant-in-Aid for a "High-Tech Research Center" Project for Private Universities, matching fund subsidy from the Ministry of Education, Culture, Sports, Science and Technology, and Scientific Research (B) and (C) from Japan Society for the Promotion of Science, and grants from the NOVARTIS Foundation (Japan) for the Promotion of Science, the Takeda Science Foundation, the Mitsubishi Pharma Foundation, and the Tokyo Biochemical Research Foundation. The costs of publication of this article were defrayed in part by the payment of page charges. This article must therefore be hereby marked "*advertisement*" in accordance with 18 U.S.C. Section 1734 solely to indicate this fact.

[S] The on-line version of this article (available at http://www.jbc.org) contains supplemental Fig. S1.

[1] To whom correspondence should be addressed: Dept. of Immunology, Juntendo University School of Medicine, 2-1-1 Hongo, Bunkyo-ku, Tokyo 113-8421, Japan. Tel.: 81-3-5802-1045; Fax: 81-3-3813-0421; E-mail: hnakano@juntendo.ac.jp.

[2] The abbreviations used are: HDAC, histone deacetylase; ChIP, chromatin immunoprecipitation; YY1, Yin Yang 1; MAL, megakaryocytic acute leukemia; MKL1, megakaryoblastic leukemia-1; RBM, RNA-binding motif protein; GPVI, platelet collagen receptor glycoprotein VI; EMSA, electrophoretic mobility shift assay; SRF, serum response factor; siRNA, small interfering RNA; TA, transcriptional activation.

Downloaded from www.jbc.org at KYOTO PREFECTURL UNIV MED on March 5, 2009

rich, SAP (SAF-A/B, Acinus, PIAS), and coiled-coil domains (7, 8). OTT-MAL encodes a fusion protein containing complete domain structures of both OTT and MAL. However, the molecular mechanism whereby this fusion protein induces leukemia is largely unknown. On the other hand, we and others have independently identified a murine homolog of MAL, referred to as BSAC and MRTF-A by functional cloning to inhibit tumor necrosis factor α-induced cell death and bioinformatics to identify related genes to myocardin, respectively (9, 10). Accumulating studies have shown that BSAC/MAL/MKL1/MRTF-A activates the promoters containing CArG boxes $(CC(A/T)_6GG)$ through associating with serum response factor (SRF) (9–11). In addition, nuclear translocation of BSAC is tightly regulated by the Rho-actin signaling pathway (12). Although *BSAC/MAL/MKL1/MRTF-A* and *SRF* are broadly expressed in various tissues, the defect of *MKL1/MRTF-A*$^{-/-}$ mice is unexpectedly restricted to the development of the mammary gland (13, 14).

Yin Yang 1 (YY1) is a ubiquitous zinc finger transcription factor that binds to many different cellular and viral promoters in a sequence-specific manner to regulate transcription (15, 16). The mechanism by which YY1 activates or represses transcription largely depends on the interaction with other transcription factors or histone modification enzymes including TBP, TAFs, SP1, p300, and HDACs (15, 16). Importantly, the targeted disruption of *YY1* resulted in preimplantation lethality, indicating that YY1 is essential for mouse embryo development (17). Moreover, subcellular localization of YY1 is regulated in a cell cycle-dependent fashion and modulates the function of the cell cycle control genes including *Rb* and *p53*. Furthermore, a recent study has revealed that perturbed expression of YY1 inhibits maturation of granulocytes, suggesting an intimate link with the development of acute myeloid leukemia (18). Collectively, YY1 potentially controls the expression of vast array of genes that are important in basic cellular processes such as DNA replication, transcription, and cell cycle control and also involved in the leukemogenesis.

Given that the promoters containing CArG boxes are found in immediate early genes or muscle-specific genes and OTT-BSAC is involved in the development of leukemia, we speculated that OTT-BSAC activates promoter(s) containing a motif other than CArG box. We found that OTT-BSAC strongly activated the promoters of human platelet collagen receptor glycoprotein VI (*GPVI*) gene. Deletion and mutation analysis revealed that OTT-BSAC-mediated transcriptional activity depended on the YY1-binding sequences. Interestingly, in contrast to BSAC, which predominantly localized in the cytoplasm and the nuclear translocation of which is tightly regulated by the Rho-dependent signals (12), OTT and OTT-BSAC exclusively localized in the nucleus. The constitutive nuclear accumulation of OTT-BSAC may contribute to a significant enhancement of its transcriptional activity. Moreover, OTT interacted with HDAC3, and this interaction was abolished in OTT-BSAC. Collectively, these functional and spatial alterations of OTT and BSAC may culminate in the development of leukemia.

EXPERIMENTAL PROCEDURES

Reagents and Cell Culture—Anti-FLAG (Sigma-Aldrich), anti-hemagglutinin (Roche Applied Science), anti-Myc, anti-GAL4, and anti-YY1 (Santa Cruz Biotechnology), anti-HDAC3 (Biomol), anti-β-actin (BioLegend) antibodies, control mouse IgG (BD Biosciences), and control rabbit IgG (Sigma-Aldrich) were purchased from the indicated sources. HEK293 and HEK293T cells were cultured in high glucose Dulbecco's modified Eagle's medium containing 10% fetal calf serum. Megakaryocytic leukemic cell lines, CMS and CMY (T. Sato), and MEG-01 cells (M. Seto) (19) were kindly provided and cultured in RPMI1640 medium containing 10% fetal calf serum. Anti-OTT antibody was generated by immunizing rabbits with GST-OTT (609–730). Anti-BSAC antibody was generated and described previously (9).

Plasmids—pBJ5-FLAG-HDAC1 (S. Schreiber), pME18S-FLAG-HDAC2 and pCEP4-FLAG-HDAC3 (E. Seto), and pCMX-mSMRTα-FL (R. M. Evans) were kindly provided from the indicated researchers. pCR-FLAG-YY1 was constructed by PCR using pCR-YY1 as a template (20). pCR-FLAG-HDAC3ΔN and pCR-FLAG-HDAC3ΔC were constructed by deleting N-terminal 307 and C-terminal 121 amino acids using PCR, respectively. A full-length *OTT* cDNA was isolated by screening a library derived from human HTLV-1-transformed T cell line HAT109 as a standard procedure. To express full-length and various deletion mutants of OTT as fusion proteins with DNA-binding domain of a yeast transcriptional factor GAL4, PCR products encoding the indicated amino acids were subcloned into pFA vector (Stratagene), designated as pFA-OTT, pFA-OTT(1–677), pFA-OTT(654–957), pFA-OTT(609–730), and pFA-OTT(1–533). pcDNA3-Myc-OTT was constructed by PCR and subcloned into pcDNA3-Myc vector. pcDNA3-Myc-human BSAC and pCR-FLAG-human HDAC6 were constructed by PCR using KIAA1438 (human *BSAC/MAL/MKL1/MRTF-A*) and KIAA0901 (human *HDAC6*) cDNAs derived from the Kazusa DNA Institute as templates, respectively. To make an expression vector for OTT-BSAC, PCR products of *OTT* and *BSAC* were connected by creating an additional EcoRI site at the fusion junction and ligated to pcDNA3-Myc vector. The artificially created EcoRI site was subsequently mutated to the originally published sequence of the *OTT-BSAC* fusion junction using a QuikChange site-directed mutagenesis kit (Stratagene). Expression vectors for C-terminal deletion mutants of OTT-BSAC (−351) and OTT-BSAC (−537) were constructed by using the internal restriction enzyme sites XmnI and BsgI to delete C-terminal fragments, respectively. The numbers indicate deleted amino acids from the C terminus of OTT-BSAC.

Reporter Assay—The promoter of the human *GPVI* gene (−315 to +29) was amplified by PCR using human genomic DNA as a template and subcloned into pGL3-basic vector (Promega), designated as pGL3-*GPVI* (−315/+29). A series of 5′ deletion mutants, pGL3-*GPVI* (−207/+29), pGL3-*GPVI* (−79/+29), and pGL3-*GPVI* (−39/+29) were generated by PCR using pGL3-*GPVI* (−315/+29) as a template. pGL3-*GPVI* (−208/+29M1), pGL3-*GPVI* (−208/+29M2), and pGL3-*GPVI* (−79/+29M3) were generated by introducing mutations

Downloaded from www.jbc.org at KYOTO PREFECTURL UNIV MED on March 5, 2009

of GATA (AGATAA to CGCTTA), the first YY1 (GATGAG to GCTTAG), and third YY1 (CTCATC to CTAAGC) binding sites, respectively. Reporter plasmids, pGL3-c-*fos* (−700/+53), pGL3-*FcεRIα* (−605/+29), and mPGV-B-*il-6* (−181/+14) were described previously (9, 20, 21). Luciferase assays using HEK293 and HEK293T cells were performed as previously described (22). MEG-01 cells (2×10^5) were transfected with the indicated expression vectors along with reporter plasmids using Lipofectamine 2000 (Invitrogen). After 48 h, the cells were harvested, and the luciferase activities were measured on a luminometer (Berthold).

Electrophoretic Mobility Shift Assay (EMSA)—EMSA was performed as previously described (20). Briefly, 5 μg of the nuclear extracts were incubated with the rhodamine-labeled wild-type oligonucleotides in the absence or presence of anti-YY1 antibody, wild-type, or mutant cold competitors with a 10–100-fold excess. The oligonucleotides used were as follows: wild-type sense oligonucleotide for *GPVI*, 5′-AGGAAGGGAGGAGAGCATTCTTCATCCTCATCACATCCTG-3′; mutant sense oligonucleotide, 5′-AGGAAGGGAGGAGAGCATTCTTCATCCTAAGCGCATCCTG-3′. Mobility shift of the complexes was analyzed by a fluorescence detector, FMBIO-100 (Takara Shuzo).

Chromatin Immunoprecipitation (ChIP) Assay—The ChIP assay was performed using a ChIP Assay kit (Millipore) as previously described (23). Quantitative PCRs were performed using TaqMan Universal PCR master mix and a 7500 Real-Time PCR system (Applied Biosystems). The primers to amplify the promoter region of *GPVI* gene (−127/+29) and a TaqMan probe were as follows: Forward primer (5′-GGCTACGGCTCGATGAGTCTC-3′), reverse primer (5′-TCAGCCCTGTCCTGAGCTCT-3′), and a TaqMan probe (5′-FAM-TTCATCCTCATCACATCC-MGB-3′). The amount of target DNA bound to YY1 or OTT-BSAC was quantified using immunoprecipitates with control, anti-YY1, or anti-Myc antibodies from the cycle threshold value, which was determined using 7500 SDS software (Applied Biosystems). In brief, the ratio of the amount of a specific DNA fragment in each immunoprecipitate to the amount of that fragment in the DNA before immunoprecipitation (input DNA) was calculated from each cycle threshold value.

Subcellular Fractionation, Immunoprecipitation, and Immunoblotting—HEK293 cells (4×10^6) were transiently transfected with the indicated expression vectors using Lipofectamine (Invitrogen). MEG-01 cells (4×10^6) were untreated or transfected with the indicated expression vectors using a nucleofector according to the manufacturer's instructions (Amaxa). For subcellular fractionation, the cells were harvested at 24–36 h after transfection and washed with 1 ml of a buffer A (10 mM Hepes, pH 7.9, 1.5 mM $MgCl_2$, 10 mM KCl, 1 μg/ml aprotinin, 1 μg/ml leupeptin, 1 mM dithiothreitol, and 1 mM phenylmethylsulfonyl fluoride) and then resuspended in 500 μl of the buffer A. After incubation for 30 min, the cells were passed with a 30-gauge syringe 10 times, followed by centrifugation at 700 × *g*. The supernatants were further centrifuged at 15,000 × *g* to remove insoluble pellets, and the resulting supernatants were collected as the cytoplasmic fractions. The pellets were resuspended in 100 μl of buffer B (20 mM Hepes, pH 7.9, 450 mM NaCl, 1.5 mM $MgCl_2$, 25% glycerol, 0.2 mM EDTA, 1 μg/ml aprotinin, 1 μg/ml leupeptin, 1 mM dithiothreitol, and 1 mM phenylmethylsulfonyl fluoride) for 60 min. After centrifugation at 15,000 × *g* for 10 min, the supernatants were collected as the nuclear fractions. Equal amounts of proteins from each fraction were subjected to SDS-PAGE and transferred onto polyvinylidine difluoride membranes (Millipore). The membranes were incubated with the indicated antibodies followed by the corresponding secondary antibodies. The membranes were then developed with the ECL Western Blotting Detection System Plus (GE Healthcare).

Small Interfering RNAs (siRNAs)—HEK293T cells (2.5×10^5) were transfected with siRNAs targeting green fluorescent protein (control) or *YY1* (ON-TARGETplus SMARTpool siRNA, Dharmacon) and pGL3-*GPVI* (−315/+29) along with Myc-OTT-BSAC using Lipofectamine 2000 (Invitrogen). After 48 h, knockdown of YY1 was evaluated by immunoblotting with anti-YY1 antibody using total lysates, and luciferase assay was performed as previously described (22).

Immunostaining—MEG-01 cells (4×10^6) were untreated or transfected with the indicated expression vectors and plated on glass slides. After 24 h, the cells were washed with phosphate-buffered saline, fixed with 2% paraformaldehyde, and then incubated with anti-OTT, anti-BSAC, and anti-Myc antibodies. The primary antibodies were detected by secondary antibodies conjugated with Alexa 488 or Alexa 594 (Invitrogen). To visualize the nuclei, the cells were incubated with Hoechst 33258 (Invitrogen). Stained cells were mounted in SlowFade (Invitrogen) and analyzed on a laser scanning confocal microscope (Zeiss).

RESULTS

Identification of a Novel Target Gene Activated by the Fusion Protein OTT-BSAC—OTT-MAL encodes a fusion protein containing complete domain structures of both OTT and MAL (Fig. 1*A*). However, the molecular mechanism whereby this fusion protein induces leukemia is largely unknown. Given that CArG boxes are found in the promoters of immediate early genes or muscle-specific genes, we speculated that OTT-BSAC should control gene(s) that might be responsible for the development of leukemia. Given that OTT-BSAC might impair the differentiation of megakaryocytes, we first tested whether OTT-BSAC could affect the promoter activity of megakaryocyte-specific genes. A previous study has shown that *GPVI* is specifically expressed in megakaryocytes and platelets (24). Then we generated a reporter plasmid containing the *GPVI* promoter upstream of a luciferase gene. We transfected megakaryocytic leukemic cell line MEG-01 cells with expression vectors for BSAC, OTT, and OTT-BSAC along with a reporter plasmid, pGL3-*GPVI* (−315/+29), and tested the effect of each protein on this promoter activity. Expression of BSAC or OTT did not significantly increase this promoter activity (Fig. 1*B*), which is consistent with the fact that this promoter does not contain a CArG box. Surprisingly, expression of OTT-BSAC strongly activated this promoter in a dose-dependent fashion (Fig. 1*B*). This OTT-BSAC-mediated transcriptional activation of the *GPVI* promoter was also observed in HEK293 cells (Fig. 1*B*). To investigate whether OTT-BSAC-dependent transcriptional activity on the *GPVI* promoter is

Downloaded from www.jbc.org at KYOTO PREFECTURL UNIV MED on March 5, 2009

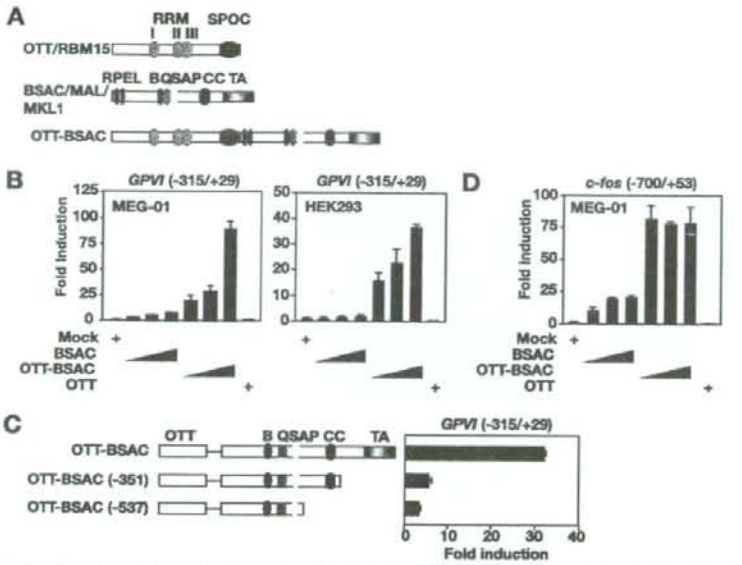

FIGURE 1. **OTT-BSAC strongly activates the *GPVI* and c-*fos* promoters.** *A*, a diagram of domain structures of OTT/RBM15, BSAC/MAL/MKL1/MRTF-A, and OTT-BSAC. RNA recognition motif, SPOC, RPEL, basic (*B*), glutamine-rich (*Q*), SAP, coiled-coil (*CC*), and TA domains are shown. *B*, MEG-01 and HEK293 cells were transfected with increasing amounts of the indicated expression vectors along with pGL3-*GPVI* (−315/+29). Luciferase activities are expressed as fold increases above that with control vector. Each experiment was performed in triplicate, and the results are expressed as the means ± SE of three experiments. *C*, MEG-01 cells were transfected activities are expressed as in *B*. *D*, MEG-01 cells were transfected with increasing amounts of the indicated expression vectors along with pGL3-c-*fos* (−700/+53). Luciferase activities are expressed as in *B*.

mediated by the transcriptional activation (TA) domain of BSAC, we transfected MEG-01 cells with deletion mutants of OTT-BSAC lacking the TA domain. Although the expression levels of two OTT-BSAC mutants lacking the TA domain were comparable with OTT-BSAC (supplemental Fig. S1), two mutants failed to activate this promoter (Fig. 1*C*). This indicates that the TA domain of BSAC mediates transcriptional activity of OTT-BSAC. Given that protein expression levels of OTT-BSAC were consistently lower than BSAC, possibly because of its large molecular mass of OTT-BSAC (supplemental Fig. S1), increased transcriptional activity of OTT-BSAC is not due to the increased protein expression levels. Consistent with a previous study (11), we also observed significant enhancement of transcriptional activity of OTT-BSAC on the c-*fos* promoter compared with BSAC (Fig. 1*D*). Given that the *GPVI* but not c-*fos* promoter does not contain CArG box, these results suggest that OTT may directly or indirectly recruit BSAC to the *GPVI* promoter, resulting in up-regulation of the *GPVI* promoter activity.

Transcriptional Activation by OTT-BSAC Depends on the YY1-binding Sequences—To identify a target sequence recognized by OTT-BSAC, we constructed a series of 5′ deletion mutants of the *GPVI* promoter (Fig. 2*A*). Although deletion up to the position −208 did not impair the transcriptional activity induced by OTT-BSAC, further deletion up to −80 reduced the transcriptional activity to ~50% (Fig. 2*B*). Moreover, deletion up to −40 resulted in complete loss of the transcriptional activation. These results indicate that the regions spanning −207 to −80 and −79 to −40 are essential for OTT-BSAC-mediated transactivation. A previous study has shown that the *GPVI* promoter activity is regulated by Sp1, GATA, and Ets motifs (24). In addition, we found three putative YY1-binding sequences (designated as YY1-I, YY1-II, and YY1-III) in the *GPVI* promoter (Fig. 2*A*). We tested whether the mutation of these sites impairs OTT-BSAC-mediated transactivation. The mutation of the GATA-binding sequence did not reduce but rather enhanced the transcriptional activity. Unexpectedly, mutation of YY1-I reduced the transcriptional activity comparable with a deletion mutant (−79/+29) (Fig. 2*B*). Furthermore, the mutation of YY1-III substantially reduced the transcriptional activity 5-fold. Notably, combined mutations of YY1-III along with Ets motifs or YY1-II did not further reduce the transcriptional activity compared with YY1-III mutation alone (data not shown). Combining these data together indicates that YY1-I and YY1-III sequences are essential for OTT-BSAC-dependent transcriptional activation.

We next tested whether YY1 actually binds to the promoter by EMSA. We prepared the nuclear extracts from MEG-01 cells and performed EMSA using double-stranded oligonucleotides (oligonucleotides) containing a region spanning −79 to −40 as a probe. As shown in Fig. 2*C*, two major retarded bands (designated the complex I and II hereafter) were detected in this assay, and these two bands disappeared by the addition of the nonlabeled wild-type oligonucleotides. In contrast, the addition of the mutant probe, in which YY1-binding core sequence (TCAT) was mutated to TAAG, did not abolish the binding of the two complexes to the labeled oligonucleotides, indicating that these complexes specifically bound to TCAT sequence. Moreover, complex II but not complex I disappeared in the presence of anti-YY1 antibody, suggesting that complex II contains YY1. Collectively, YY1 binds to the *GPVI* promoter via TCAT sequence. However, we could not detect direct interaction of YY1 with BSAC or OTT in cotransfection experiments or a ternary complex containing YY1 and BSAC or OTT-BSAC in the presence of YY1-binding sequence in EMSAs (data not shown).

To directly show that endogenous YY1 is recruited to the *GPVI* promoter under more physiological conditions, we performed ChIP assays. Consistent with EMSAs, anti-YY1 but not control antibody efficiently immunoprecipitated the *GPVI* promoter from HEK293T and MEG-01 cells (Fig. 2*D*). However, the relative intensities of the *GPVI* promoter using immunoprecipitates with anti-Myc antibody were not different in between mock and Myc-OTT-BSAC-transfected HEK293T cells (Fig. 2*E*). This suggests that the recruitment of transfected

Downloaded from www.jbc.org at KYOTO PREFECTURL UNIV MED on March 5, 2009

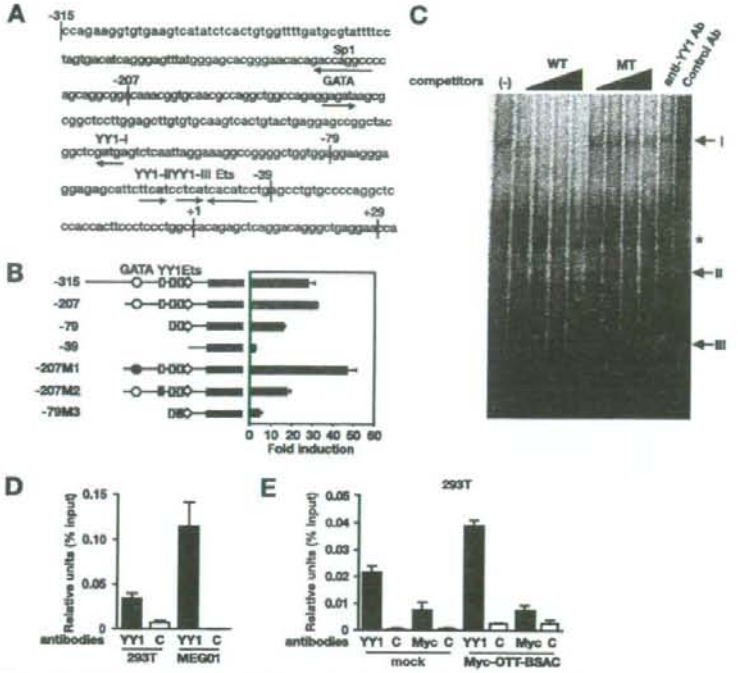

FIGURE 2. **OTT-BSAC activates the *GPVI* promoter via the YY1-binding motifs.** *A*, the promoter region of human *GPVI* gene. The putative transcriptional factor binding sites are *underlined* by the *arrows* showing its orientation (sense or antisense orientation). *+1* indicates the transcription start site. The putative YY1-binding sequences are indicated by *bold characters*. *B*, delineation of the regions required for OTT-BSAC-dependent transactivation. MEG-01 cells were transfected with OTT-BSAC along with the indicated mutants of pGL3-*GPVI* reporter vector. Luciferase activities are expressed as in Fig. 1*B*. *M1*, *M2*, and *M3* are the mutants, in which GATA1, the first YY1, and third YY1 motifs were mutated, respectively. *C*, YY1 specifically binds to the promoter of *GPVI*. The nuclear extracts were incubated with the rhodamine-labeled wild-type oligonucleotides containing the *GPVI* promoter (−79 to −39) in the absence or presence of increasing amounts of the nonlabeled wild-type (*WT*) or mutant (*MT*) oligonucleotides or anti-YY1 or control antibodies. The retarded bands are indicated by *arrows*. The *asterisk* indicates nonspecific bands. *D*, *in vivo* binding of YY1 to the *GPVI* promoter in HEK293T and MEG-01 cells. The binding of YY1 to the *GPVI* promoter region (−127/+22) was quantified using ChIP assays. The results are expressed as the means ± S.D. of three independent PCRs with duplicates samples. *E*, OTT-BSAC does not bind to the *GPVI* promoter *in vivo*. Mock or Myc-OTT-BSAC-transfected HEK293T cells were subjected to ChIP assays using anti-YY1, anti-Myc, or control antibodies. The results are expressed as in *D*.

OTT-BSAC to the *GPVI* promoter could not be detected, at least under our experimental conditions.

YY Is Not Essential for OTT-BSAC-dependent Transcriptional Activation—Previous studies have shown that myocardin and BSAC do not directly bind to the promoters containing CArG boxes but activates them through interaction with SRF (9–11). Under these conditions, transcriptional activities by myocardin and BSAC are extremely sensitive to the levels of SRF, because high concentration of SRF does not enhance but rather attenuates myocardin- or BSAC-dependent transcriptional activation (25).[3] To test whether similar interplay between OTT-BSAC and YY1 is also observed on the *GPVI* promoter, we examined whether expression of YY1 attenuates OTT-BSAC-dependent transactivation. Although expression of YY1 alone weakly activated this promoter, expression of YY1 substantially inhibited OTT-BSAC-mediated transcriptional activation in a dose-dependent fashion (Fig. 3*A*). Notably, this inhibitory effect of YY1 was promoter-specific, because expression of YY1 only weakly inhibited OTT-BSAC-dependent transactivation on the *c-fos* promoter (Fig. 3*B*). We confirmed that the expression levels of transfected YY1 in the *GPVI* promoter-transfected MEG-01 cells were nearly identical to those of *c-fos* promoter-transfected MEG-01 cells (Fig. 3*C*).

The fact that YY1 substantially suppressed OTT-BSAC-mediated transcriptional activation raises two possibilities. One is that YY1 may recruit OTT-BSAC to the *GPVI* promoter, although the recruitment of transfected OTT-BSAC to the *GPVI* promoter was not detected under our experimental conditions (Fig. 2*E*). The other is that a transcription factor other than YY1 recruits OTT-BSAC to the YY1-binding sequences and activates the *GPVI* promoter; therefore YY1 appears to suppress OTT-BSAC-dependent transcriptional activation through competitive binding inhibition (Fig. 3*A*). To discriminate these two possibilities, we knocked down endogenous YY1 using siRNA and tested whether OTT-BSAC-dependent transcriptional activation is abolished in YY1-knockdown HEK293T cells. Although *YY1* siRNA efficiently knocked down expression of YY1, OTT-BSAC-mediated transcriptional activation was not impaired (Fig. 3*D*). Collectively, OTT-BSAC activates transcription on the *GPVI* promoter through the YY1-binding sequences, but YY1 is not essential for OTT-BSAC- mediated transcriptional activation.

We finally investigated whether OTT-BSAC activates other promoters containing the YY1-binding sequences. We have previously shown that the human *FcεRIα* subunit promoter contains the YY1-binding sequences and is activated by YY1 (20). Thus, we tested whether expression of OTT-BSAC activates this promoter. As expected, OTT-BSAC substantially increased this promoter activity (Fig. 3*E*). We also found that OTT-BSAC activates the murine *il-6* promoter, which also contains the YY1-binding sequences (Fig. 3*E*).

The Signal-independent Nuclear Accumulation of OTT-BSAC—To elucidate the mechanism whereby transcriptional activity of OTT-BSAC is enhanced compared with BSAC, we speculated that OTT fusion to BSAC could affect the subcellular localization of BSAC. We first examined the subcellular

[3] T. Sawada and H. Nakano, unpublished results.

Downloaded from www.jbc.org at KYOTO PREFECTURL UNIV MED on March 5, 2009

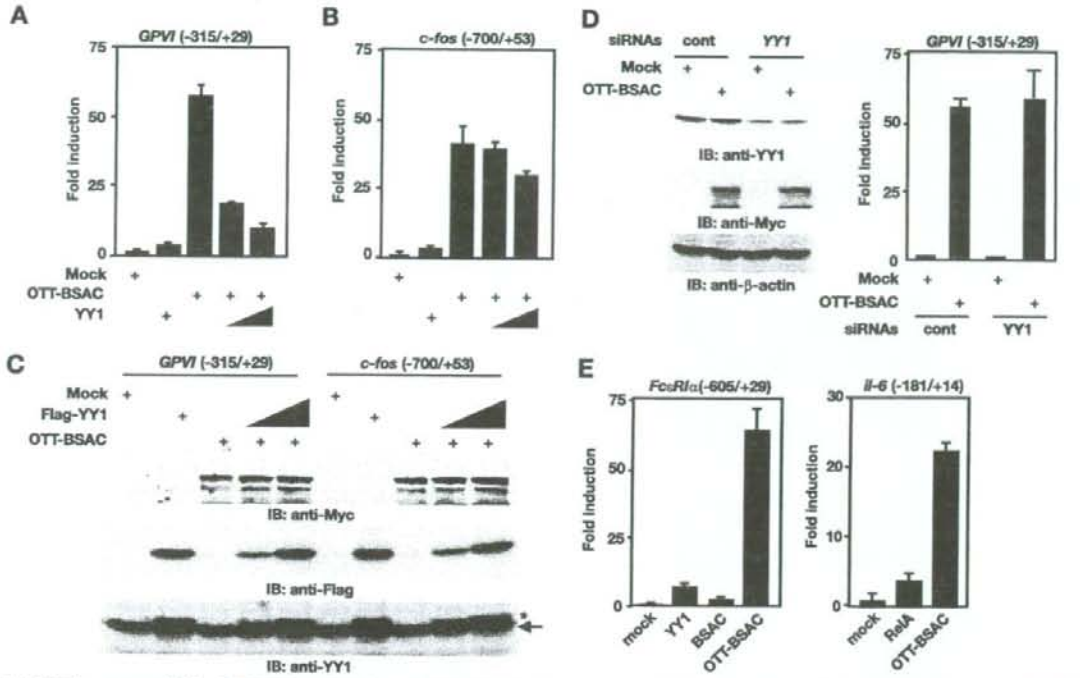

FIGURE 3. **YY is not essential for OTT-BSAC-mediated transcriptional activation.** *A–C*, MEG-01 cells were transfected with Myc-OTT-BSAC and pGL3-*GPVI* (−315/+29) (*A* and *C*) or pGL3-*c-fos* (−700/+53) (*B* and *C*) along with increasing amounts of FLAG-YY1. The luciferase activities are expressed as in Fig. 1*B*. *C*, expression levels of transfected proteins and endogenous YY1 were detected by immunoblotting (*IB*) with anti-Myc, anti-FLAG, and anti-YY1 antibodies. The *arrow* and *asterisk* indicate endogenous and transfected YY1, respectively. *D*, knockdown of YY1 using siRNA does not impair OTT-BSAC-dependent transcriptional activation. HEK293T cells were transfected with siRNAs targeting green fluorescent protein (control) or *YY1* and pGL3-*GPVI* (−315/+29) along with an empty vector (mock) or Myc-OTT-BSAC. After 48 h, the expression levels of endogenous YY1 and transfected OTT-BSAC were detected by immunoblotting with anti-YY1 (*top panel*) and anti-Myc antibodies (*middle panel*), respectively. The equal loading of the samples was verified by immunoblotting with anti-β-actin antibody (*bottom panel*). The luciferase activities are expressed as in Fig. 1*B*. *E*, MEG-01 cells were transfected with the indicated expression vectors along with pGL3-*FcεRIα* (−605/+29) or mPGV-B-*Il-6* (−181/+14). The luciferase activities are expressed as in Fig. 1*B*.

localization of endogenous BSAC and OTT in MEG-01 cells. Consistent with a previous study (12), endogenous BSAC predominantly localized in the cytoplasm with a minor population in the nucleus (Fig. 4*A*). To investigate the subcellular localization of endogenous OTT, we generated anti-OTT antibody. This antibody recognized endogenous OTT with a molecular mass of 120 kDa in the whole cell lysates from MEG-01, HeLa, HEK293, and Jurkat T, but not CMS or CMY cells (Fig. 4*C*). Consistent with a very recent study, in which ectopically expressed OTT localizes in the nucleus (26), endogenous OTT localized in the nucleus (Fig. 4*A*). Similarly, transfected BSAC and OTT showed identical subcellular distribution patterns to endogenous BSAC and OTT, respectively (Fig. 4*B*). We finally investigated the localization of OTT-BSAC. Because leukemia cell line(s) from patients with acute megakaryoblastic leukemia are not currently available, we transiently transfected MEG-01 cells with Myc-OTT-BSAC. Interestingly, OTT-BSAC exclusively localized in the nucleus (Fig. 4*B*).

To evaluate the subcellular localization of OTT, BSAC, and OTT-BSAC more quantitatively, we separated the cells into the cytoplasmic and nuclear fractions and detected each protein in the fractions by using Western blotting. Consistent with the results using a confocal microscopy, endogenous and transfected OTT mainly localized in the nucleus (Fig. 4, *D* and *E*). Although endogenous and transfected BSAC predominantly localized in the cytoplasm and the small population of BSAC localized in the nucleus, transfected OTT-BSAC exclusively localized in the nucleus. Collectively, OTT fusion to BSAC drastically changed the subcellular localization of BSAC. This might be one of the molecular mechanisms underlying the aberrant up-regulation of OTT-BSAC-dependent transcriptional activity.

OTT Interacts with HDAC3—A previous study has shown that SHARP interacts with HDACs, SMRT, and N-CoR and acts as a transcriptional repressor (5). OTT has a structural similarity to SHARP (5, 6), prompting us to test whether OTT interacts with HDACs. We transiently transfected HEK293 cells with Myc-OTT along with FLAG-HDAC1, -2, or -3. The lysates were immunoprecipitated with anti-Myc antibody, and co-immunoprecipitated HDACs were detected by anti-FLAG antibody. HDAC3, but not HDAC1 or HDAC2, was specifically co-immunoprecipitated with OTT (Fig. 5*A*). In contrast, BSAC could not bind to HDAC3. A reciprocal immunoprecipitation experiment showed that OTT was also co-immunoprecipitated with HDAC3 (Fig. 5*A*). On the other hand, OTT did not interact with HDAC6, a member of the class II HDAC family (data

Downloaded from www.jbc.org at KYOTO PREFECTURL UNIV MED on March 5, 2009

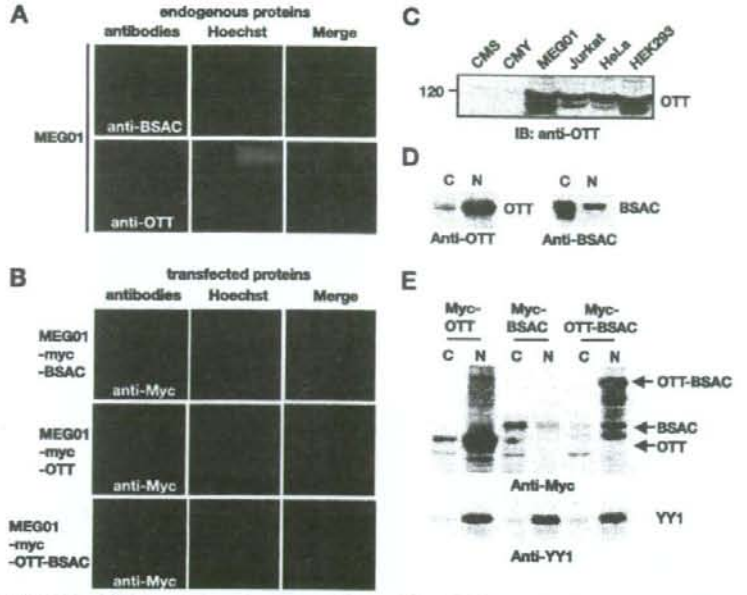

FIGURE 4. **Signal-independent nuclear accumulation of OTT-BSAC.** *A* and *B*, MEG-01 cells were untransfected (*A*) or transfected (*B*) with Myc-BSAC, Myc-OTT, or Myc-OTT-BSAC. Then the cells were stained with anti-BSAC (*A*), anti-OTT (*A*), or anti-Myc (*B*) antibodies and analyzed by a confocal microscopy. The nuclei were stained with Hoechst 33258 (*blue*) and the merged images are represented at the *right*. *C*, expression of OTT in various cell lines. Expression levels of endogenous OTT were analyzed by immunoblotting (*IB*) with anti-OTT antibody. The relative molecular mass (kDa) is indicated at the *left*. *D*, subcellular fractionation of endogenous OTT and BSAC in MEG-01 cells. Subcellular fractionation was performed as described under "Experimental Procedures," and equal amounts of proteins were subjected to SDS-PAGE. The expression levels of OTT and BSAC were analyzed by immunoblotting with anti-OTT and anti-BSAC antibodies, respectively. *C* and *N* indicate the cytosolic and nuclear fractions, respectively. *E*, subcellular localization of transfected Myc-OTT, Myc-BSAC, and Myc-OTT-BSAC. MEG-01 cells were transfected with the indicated vectors, and the subcellular fractionation and SDS-PAGE were performed as in *D*. Expression levels of transfected proteins in each fraction were analyzed by immunoblotting with anti-Myc antibody (*top panel*). The equal loading of the nuclear extracts was verified by immunoblotting with anti-YY1 antibody (*bottom panel*).

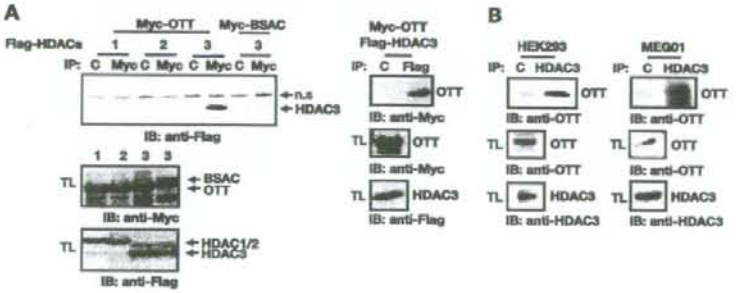

FIGURE 5. **OTT physically interacts with HDAC3.** *A*, OTT interacts with HDAC3, but not HDAC1 or HDAC2. HEK293 cells were transfected with the indicated expression vectors. After immunoprecipitation (*IP*) with control (*lane C*), anti-Myc, or anti-FLAG antibodies, co-immunoprecipitated proteins were detected by immunoblotting (*IB*) with anti-FLAG or anti-Myc antibodies (*top panel*). Expression levels of the transfected proteins in the total lysates (*TL*) were analyzed by immunoblotting with anti-Myc or anti-FLAG antibodies, respectively (*middle* and *bottom panels*). The *numbers 1*, *2*, and *3* indicate HDAC1, HDAC2, and HDAC3, respectively. *B*, endogenous interaction of OTT with HDAC3 in HEK293 and MEG-01 cells. After immunoprecipitation with control (*lane C*) or anti-HDAC3 antibodies, co-immunoprecipitated OTT was detected by immunoblotting with anti-OTT antibody (*top panels*). Expression levels of endogenous OTT and HDAC3 in the total lysates were analyzed by immunoblotting with anti-OTT and HDAC3 antibodies, respectively (*middle* and *bottom panels*).

not shown). To confirm the interaction of OTT with HDAC3 under more physiological conditions, we immunoprecipitated the lysates from HEK293 and MEG-01 cells with anti-HDAC3 antibody, and then co-immunoprecipitated OTT was detected with anti-OTT antibody. Anti-HDAC3, but not control antibody efficiently co-immunoprecipitated endogenous OTT (Fig. 5*B*). Collectively, these results indicate that OTT physically interacts with HDAC3 *in vivo*.

It is well known that HDAC3 is a component of a large nuclear corepressor complex including Sin3A, N-CoR, and SMRT. We next tried to detect interaction of OTT with Sin3A, N-CoR, and SMRT; however, under our experimental conditions, we could not detect direct interaction of OTT with either of them (data not shown). Therefore, future study will be required to address whether OTT might be a component of the nuclear corepressor complex.

Domain Mapping of OTT and HDAC3 for Their Interaction—We next delineated the regions of HDAC3 and OTT responsible for their interaction. Co-immunoprecipitation experiments using deletion mutants of HDAC3 revealed that N-terminal 307 amino acids were sufficient for binding to OTT (Fig. 6, *A* and *B*). Because the expression levels of HDAC3ΔN were consistently very low because of an increase in sensitivity to degradation of the transfected HDAC3ΔN in the cells, we could not formally exclude the possibility that HDAC3ΔN may also mediate the interaction of HDAC3 with OTT.

To determine the binding region of OTT to HDAC3, we constructed a series of deletion mutants of OTT and expressed them as fusion proteins with the DNA-binding domain of GAL4 (Fig. 6*C*). Although a region containing 609–730 amino acids could not bind to HDAC3, the N-terminal region containing three RNA recognition motifs and the C-terminal SPOC domains independently bound to HDAC3 (Fig. 6*D*), indicating that OTT interacts with HDAC3 via multiple regions.

OTT-BSAC Does Not Interact with HDAC3—We next investigated whether BSAC fusion to OTT could affect the ability to

Downloaded from www.jbc.org at KYOTO PREFECTURL UNIV MED on March 5, 2009

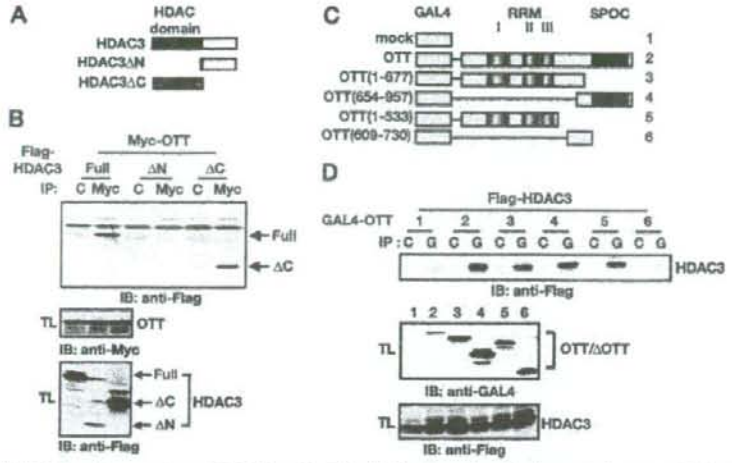

FIGURE 6. **Domain mapping of HDAC3 and OTT for their interaction.** *A*, schematic diagrams of deletion mutants of HDAC3. *B*, N-terminal HDAC domain is responsible for the binding to OTT. HEK293 cells were transfected with the indicated mutants of HDAC3 along with Myc-OTT. After immunoprecipitation (*IP*) with control (*lane C*) or anti-Myc antibodies, co-immunoprecipitated proteins were detected by immunoblotting (*IB*) with anti-FLAG antibody (*top panel*). Expression levels of transfected proteins (*TL*) were analyzed as in Fig. 5*A* (*middle* and *bottom panels*). *C*, schematic diagrams of deletion mutants of OTT fused to the DNA-binding domain of GAL4. *D*, OTT interacts with HDAC3 via multiple regions. HEK293 cells were transfected with the indicated mutants of GAL4-OTT along with FLAG-HDAC3. After immunoprecipitation with control (*lanes C*) or anti-GAL4 (*lanes G*) antibodies, co-immunoprecipitated proteins were detected by immunoblotting with anti-FLAG antibody (*top panel*). Expression levels of transfected proteins (*TL*) were analyzed as in Fig. 5*A* (*middle* and *bottom panels*). The *numbers* indicate each mutant of GAL4-OTT described as in *C*.

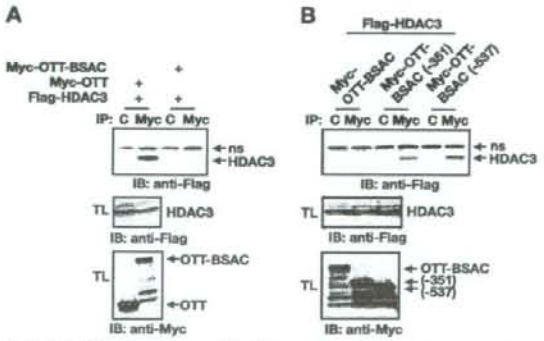

FIGURE 7. **BSAC fusion to OTT disrupts the interaction of OTT with HDAC3.** *A*, HEK293 cells were transfected with FLAG-HDAC3 along with Myc-OTT or Myc-OTT-BSAC. After immunoprecipitation (*IP*) with control (*lane C*) or anti-Myc antibodies, co-immunoprecipitated proteins were detected by immunoblotting (*IB*) with anti-FLAG antibody (*top panel*). Expression levels of the transfected proteins in the total lysates (*TL*) were analyzed as in Fig. 5*A* (*middle* and *bottom panels*). *ns* indicates nonspecific bands. *B*, HEK293 cells were transfected with FLAG-HDAC3 along with the indicated deletion mutants of Myc-OTT-BSAC. Immunoprecipitation and Western blotting were performed as in Fig. 5*A*.

interact with HDAC3. Interestingly, OTT-BSAC lost the ability to interact with HDAC3 (Fig. 7*A*). Given that the domain structure of OTT is preserved in OTT-BSAC, this suggests that some region of BSAC could inhibit the interaction of OTT with HDAC3. To determine the inhibitory region, we constructed C-terminal deletion mutants of OTT-BSAC (Fig. 7*B*). Deletion of C-terminal 351 amino acids containing the TA domain of OTT-BSAC restored the binding to HDAC3, suggesting that the C-terminal TA domain inhibits the binding of HDAC3 to OTT.

DISCUSSION

In the present study, we have shown that a fusion protein OTT-BSAC exhibited strong transcriptional activity to various promoters containing the YY1-binding sequences. Although BSAC predominantly localized in the cytoplasm, OTT-BSAC exclusively localized in the nucleus. This signal-independent nuclear accumulation of OTT-BSAC might contribute to a significant enhancement of transcriptional activity. Moreover, OTT interacted with HDAC3, but this interaction was abolished in OTT-BSAC. Given that OTT negatively regulates the myeloid and megakaryocyte expansion (26, 27), the loss of suppressor function of OTT along with aberrant up-regulation of BSAC-dependent transactivation caused by the fusion may culminate in the development of leukemia.

We and others have previously reported that BSAC activates the promoters containing CArG boxes through association with SRF (9–11). However, given that CArG boxes are found in the promoters of many immediate early genes or muscle-specific genes, it is unlikely that CArG box-dependent transcriptional activity of BSAC directly links to the development of leukemia. Thus, we surmised that OTT-BSAC activates a promoter containing a sequence other than the CArG box(es). We found that OTT-BSAC activated the *GPVI* promoter through YY1-binding sequences. This conclusion is supported by the following results. First, OTT-BSAC-mediated transcriptional activity was abolished on the *GPVI* promoters, in which the YY1-binding sequences were mutated (Fig. 2*B*). Second, YY1 bound to this site using EMSAs (Fig. 2*C*). Third, ChIP assays revealed that endogenous YY1 bound to the *GPVI* promoter (Fig. 2*D*). However, we could not detect the recruitment of transfected OTT-BSAC to the promoter of *GPVI* using ChIP assays under our experimental conditions (Fig. 2*E*). It is reasonable to speculate that only small populations of transfected OTT-BSAC might be recruited to the promoter; therefore such recruitment might be under the detection levels.

Although the present study has shown that OTT-BSAC activates the *GPVI* and other promoters containing the YY1-binding sequences, it remains unclear which transcriptional factor(s) is essential for OTT-BSAC-mediated transcriptional activation. Although overexpression of YY1 attenuated OTT-BSAC-dependent transcriptional activation (Fig. 3*A*), knockdown of YY1 using siRNA did not impair its transcriptional activity (Fig. 3*D*). Given that we could not detect the interaction of YY1 with OTT-BSAC (data not shown), OTT-BSAC might

Downloaded from www.jbc.org at KYOTO PREFECTURL UNIV MED on March 5, 2009

be recruited to the YY1-binding motif through interaction with a transcription factor other than YY1. Intriguingly, YY2, a member of the YY1 family, has been shown to bind to the consensus binding sequences similar to YY1 (28); YY2 may recruit OTT-BSAC to the *GPVI* promoter. Further study will be required to address this possibility.

A previous study has shown that persistent expression of YY1 in 3DO cells after differentiation signal could perturb the granulocyte differentiation (18). Moreover, up-regulation of *YY1* mRNA is frequently observed in some patients of acute myeloid leukemia (18). These results indicate an intimate link between deregulation of YY1 and leukemia. Together, OTT-BSAC might modulate YY1- and/or YY1-related transcriptional factor-dependent transcription, culminating in the development of leukemia.

Another important finding of this study is that OTT fusion to the N terminus of BSAC resulted in signal-independent nuclear accumulation of OTT-BSAC. A previous study has shown that nuclear translocation of BSAC is tightly regulated by the Rho-actin signaling pathway (12). Consistently, under unstimulated conditions, endogenous BSAC predominantly localized in the cytoplasm (Fig. 4). These results suggest that transcriptional activity of BSAC is at least partly regulated by its subcellular localization. This might well explain the reason why OTT-BSAC shows stronger transcriptional activity than BSAC. However, the mechanism by which OTT-BSAC constitutively accumulates in the nucleus remains to be solved in this study. One possible scenario is that the nuclear localization signal(s) of OTT might dominate over the cytoplasmic retention signal(s) of BSAC. Although BSAC has its own nuclear localization signals in the basic domain, N-terminal RPEL motifs are considered to sequestrate BSAC to the cytoplasm via interaction with G actin under unstimulated conditions (12). Therefore, OTT might disrupt such inhibition, resulting in constitutive nuclear translocation of OTT-BSAC.

A recent study has shown that deletion of *OTT* gene results in megakaryocytic expansion (27). In addition, knockdown of *OTT/RBM15* gene using RNA interference promotes myeloid differentiation (26), suggesting an inhibitory role for OTT in myeloid and megakaryocyte development. These results are consistent with our present study, in which OTT might act as a transcriptional repressor via interaction with HDAC3 (Fig. 6). Given that this transcriptional repressor activity of OTT might be abolished in OTT-BSAC, the loss of OTT-mediated suppressor function of OTT-BSAC along with aberrant up-regulation of BSAC-dependent transcriptional activity might synergistically contribute to the development of leukemia.

Acknowledgments—We thank Drs. Don Ayer, Edward Seto, Stuart Schreiber, Jiemin Wang, A. Gregory Materal, Ron M. Evans, the Kazusa DNA Institute, Takeyuki Sato, and Masao Seto for providing reagents and cell lines. We also thank Drs. Alan B. Cantor, Jean-Pierre Bourquin, Yuriko Suzuki, Tatsuo Fukagawa, Mitsuru Matsumoto, and Mikiko Chihara-Siomi for helpful discussion.

REFERENCES

1. Struhl, K. (1998) *Genes Dev.* **12,** 599–606
2. Ng, H. H., and Bird, A. (2000) *Trends Biochem. Sci* **25,** 121–126
3. Yang, X. J., and Gregoire, S. (2005) *Mol. Cell. Biol.* **25,** 2873–2884
4. Jepsen, K., and Rosenfeld, M. G. (2002) *J. Cell Sci.* **115,** 689–698
5. Shi, Y., Downes, M., Xie, W., Kao, H. Y., Ordentlich, P., Tsai, C. C., Hon, M., and Evans, R. M. (2001) *Genes Dev.* **15,** 1140–1151
6. Ariyoshi, M., and Schwabe, J. W. (2003) *Genes Dev.* **17,** 1909–1920
7. Mercher, T., Coniat, M. B., Monni, R., Mauchauffe, M., Khac, F. N., Gressin, L., Mugneret, F., Leblanc, T., Dastugue, N., Berger, R., and Bernard, O. A. (2001) *Proc. Natl. Acad. Sci. U. S. A.* **98,** 5776–5779
8. Ma, Z., Morris, S. W., Valentine, V., Li, M., Herbrick, J. A., Cui, X., Bouman, D., Li, Y., Mehta, P. K., Nizetic, D., Kaneko, Y., Chan, G. C., Chan, L. C., Squire, J., Scherer, S. W., and Hitzler, J. K. (2001) *Nat. Genet.* **28,** 220–221
9. Sasazuki, T., Sawada, T., Sakon, S., Kitamura, T., Kishi, T., Okazaki, T., Katano, M., Tanaka, M., Watanabe, M., Yagita, H., Okumura, K., and Nakano, H. (2002) *J. Biol. Chem.* **277,** 28853–28860
10. Wang, D. Z., Li, S., Hockemeyer, D., Sutherland, L., Wang, Z., Schratt, G., Richardson, J. A., Nordheim, A., and Olson, E. N. (2002) *Proc. Natl. Acad. Sci. U. S. A.* **99,** 14855–14860
11. Cen, B., Selvaraj, A., Burgess, R. C., Hitzler, J. K., Ma, Z., Morris, S. W., and Prywes, R. (2003) *Mol. Cell. Biol.* **23,** 6597–6608
12. Miralles, F., Posern, G., Zaromytidou, A. I., and Treisman, R. (2003) *Cell* **113,** 329–342
13. Li, S., Chang, S., Qi, X., Richardson, J. A., and Olson, E. N. (2006) *Mol. Cell. Biol.* **26,** 5797–5808
14. Sun, Y., Boyd, K., Xu, W., Ma, J., Jackson, C. W., Fu, A., Shillingford, J. M., Robinson, G. W., Hennighausen, L., Hitzler, J. K., Ma, Z., and Morris, S. W. (2006) *Mol. Cell. Biol.* **26,** 5809–5826
15. Shi, Y., Lee, J. S., and Galvin, K. M. (1997) *Biochim. Biophys. Acta* **1332,** 49–66
16. Thomas, M. J., and Seto, E. (1999) *Gene (Amst.)* **236,** 197–208
17. Donohoe, M. E., Zhang, X., McGinnis, L., Biggers, J., Li, E., and Shi, Y. (1999) *Mol. Cell. Biol.* **19,** 7237–7244
18. Erkeland, S. J., Valkhof, M., Heijmans-Antonissen, C., Delwel, R., Valk, P. J., Hermans, M. H., and Touw, I. P. (2003) *Blood* **101,** 1111–1117
19. Ogura, M., Morishima, Y., Ohno, R., Kato, Y., Hirabayashi, N., Nagura, H., and Saito, H. (1985) *Blood* **66,** 1384–1392
20. Nishiyama, C., Hasegawa, M., Nishiyama, M., Takahashi, K., Akizawa, Y., Yokota, T., Okumura, K., Ogawa, H., and Ra, C. (2002) *J. Immunol.* **168,** 4546–4552
21. Muraoka, O., Kaisho, T., Tanabe, M., and Hirano, T. (1993) *Immunol. Lett.* **37,** 159–165
22. Nakano, H., Shindo, M., Sakon, S., Nishinaka, S., Mihara, M., Yagita, H., and Okumura, K. (1998) *Proc. Natl. Acad. Sci. U. S. A.* **95,** 3537–3542
23. Kanada, S., Nakano, N., Potaczek, D. P., Maeda, K., Shimokawa, N., Niwa, Y., Fukai, T., Sanak, M., Szczeklik, A., Yagita, H., Okumura, K., Ogawa, H., and Nishiyama, C. (2008) *J. Immunol.* **180,** 8204–8210
24. Holmes, M. L., Bartle, N., Eisbacher, M., and Chong, B. H. (2002) *J. Biol. Chem.* **277,** 48333–48341
25. Wang, D., Chang, P. S., Wang, Z., Sutherland, L., Richardson, J. A., Small, E., Krieg, P. A., and Olson, E. N. (2001) *Cell* **105,** 851–862
26. Ma, X., Renda, M. J., Wang, L., Cheng, E. C., Niu, C., Morris, S. W., Chi, A. S., and Krause, D. S. (2007) *Mol. Cell. Biol.* **27,** 3056–3064
27. Raffel, G. D., Mercher, T., Shigematsu, H., Williams, I. R., Cullen, D. E., Akashi, K., Bernard, O. A., and Gilliland, D. G. (2007) *Proc. Natl. Acad. Sci. U. S. A.* **104,** 6001–6006
28. Nguyen, N., Zhang, X., Olashaw, N., and Seto, E. (2004) *J. Biol. Chem.* **279,** 25927–25934

Downloaded from www.jbc.org at KYOTO PREFECTURL UNIV MED on March 5, 2009

Vol 455|16 October 2008|doi:10.1038/nature07399

LETTERS

Oncogenic mutations of ALK kinase in neuroblastoma

Yuyan Chen[1,2,3]*, Junko Takita[1,2,3]*, Young Lim Choi[4]*, Motohiro Kato[1,3], Miki Ohira[5], Masashi Sanada[2,3,6], Lili Wang[2,3,6], Manabu Soda[4], Akira Kikuchi[7], Takashi Igarashi[1], Akira Nakagawara[5], Yasuhide Hayashi[8], Hiroyuki Mano[4,6] & Seishi Ogawa[2,3,6]

Neuroblastoma in advanced stages is one of the most intractable paediatric cancers, even with recent therapeutic advances[1]. Neuroblastoma harbours a variety of genetic changes, including a high frequency of *MYCN* amplification, loss of heterozygosity at 1p36 and 11q, and gain of genetic material from 17q, all of which have been implicated in the pathogenesis of neuroblastoma[2–5]. However, the scarcity of reliable molecular targets has hampered the development of effective therapeutic agents targeting neuroblastoma. Here we show that the anaplastic lymphoma kinase (ALK), originally identified as a fusion kinase in a subtype of non-Hodgkin's lymphoma (NPM–ALK)[6–8] and more recently in adenocarcinoma of lung (EML4–ALK)[9,10], is also a frequent target of genetic alteration in advanced neuroblastoma. According to our genome-wide scans of genetic lesions in 215 primary neuroblastoma samples using high-density single-nucleotide polymorphism genotyping microarrays[11–14], the *ALK* locus, centromeric to the *MYCN* locus, was identified as a recurrent target of copy number gain and gene amplification. Furthermore, DNA sequencing of *ALK* revealed eight novel missense mutations in 13 out of 215 (6.1%) fresh tumours and 8 out of 24 (33%) neuroblastoma-derived cell lines. All but one mutation in the primary samples (12 out of 13) were found in stages 3–4 of the disease and were harboured in the kinase domain. The mutated kinases were autophosphorylated and displayed increased kinase activity compared with the wild-type kinase. They were able to transform NIH3T3 fibroblasts as shown by their colony formation ability in soft agar and their capacity to form tumours in nude mice. Furthermore, we demonstrate that downregulation of *ALK* through RNA interference suppresses proliferation of neuroblastoma cells harbouring mutated *ALK*. We anticipate that our findings will provide new insights into the pathogenesis of advanced neuroblastoma and that *ALK*-specific kinase inhibitors might improve its clinical outcome.

To identify oncogenic lesions in neuroblastoma, we performed a genome-wide analysis of primary tumour samples obtained from 215 neuroblastoma patients using high-density single-nucleotide polymorphism (SNP) arrays (Affymetrix GeneChip 250K *Nsp*I) (Supplementary Table 1). Twenty-four neuroblastoma-derived cell lines were also analysed (Supplementary Table 2). Interrogating over 250,000 SNP sites, this platform permits the identification of copy number changes at an average resolution of less than 12 kilobases (kb)[13,14].

Analysis of this large number of samples, consisting of varying disease stages, permitted us to obtain a comprehensive registry of genomic lesions in neuroblastoma (Supplementary Figs 1 and 2). A gain of chromosomes, often triploid or hyperploid (defined by mean copy number of >2.5), was a predominant feature of neuroblastoma genomes in the lower stages. Ploidy generally correlated with the clinical stage, where non-hyperploid cases were significantly associated with stage 4 disease ($P = 4.13 \times 10^{-5}$, trend test) (Supplementary Fig. 3 and Supplementary Table 3). 17q gains, frequently in multiple copies (3≤ copy number <5), were a hallmark of the neuroblastoma genome[4] and were found in most neuroblastoma cases. Copy number gains tended to spare chromosomes 3, 4, 10, 14 and 19 (Supplementary Figs 2 and 3). Notably, these chromosomes often had copy number losses including 1p (22.8%), 3p (8.8%), 4p (5.1%), 6q (7.0%), 10q (9.8%), 11q (19.5%), 14q (3.7%), 19p (7.4%) and 19q (5.1%), implicating the pathogenic role of 'relative' gene dosages.

After excluding known copy number variations, we identified a total of 28 loci undergoing high-grade amplifications (copy number ≥5) (Supplementary Table 4). These lesions fell into relatively small genomic segments, having a mean size of 361 kb, which accelerated the identification of gene targets in these regions (Supplementary Table 4 and Supplementary Fig. 4). The candidate gene targets included *TERT* (5p15.33), *HDAC3* (5q31.3), *IGF2* (11p15.1), *MYEOV* (11q13.3), *FGF7* (15q21.1) and *CDH13* (16q23.3). However, many of them were not recurrent but found only in a single case. Although the recurrent lesions were mostly explained by the amplification of *MYCN* at 2p24, as found in 50 out of 215 (23%) of the primary cases, we identified another peak of recurrent amplification at 2p23 (Fig. 1a), which consisted of amplicons in five primary cases and in one neuroblastoma-derived cell line, NB-1 (Supplementary Fig. 5). This peak was located at the centromeric margin of the common copy number gains in chromosome 2p, which was created by copy number gains in 109 samples mostly from non-hyperploid stage 4 cases. The minimum overlapping amplification was defined by the amplicons found in the NB-1 cell line (Supplementary Fig. 5) and contained a single gene, the anaplastic lymphoma kinase (*ALK*), which has previously been reported to be overexpressed in neuroblastoma cases[15]. Although five of the six samples showing *ALK* amplification also had *MYCN* amplification, one primary case (NT056) lacked a *MYCN* peak and the amplification was confined to the *ALK*-containing locus. In interphase fluorescent *in situ* hybridization (FISH) analysis of NB-1, *MYCN* and *ALK* loci were amplified in separate amplicons (Fig. 1b), indicating that the 2p23 amplicons containing *ALK* were unlikely to represent merely 'passenger' events of *MYCN* amplification but actively contributed to the pathogenesis of neuroblastoma.

Because an oncogene can be activated by gene amplification and/or mutation, to search for possible mutations we performed DNA heteroduplex formation analysis[16] and genomic DNA sequencing for the exons 20 to 28 of *ALK*, which encompass the juxtamembrane and kinase domains (Supplementary Table 5). In total, we identified eight nucleotide changes in 21 neuroblastoma samples, 13 out of 215

[1]Department of Pediatrics, [2]Cell Therapy and Transplantation Medicine, [3]Cancer Genomics Project, Graduate School of Medicine, The University of Tokyo, Tokyo 113-8655, Japan. [4]Division of Functional Genomics, Jichi Medical University, Toguchi 329-0498, Japan. [5]Division of Biochemistry, Chiba Cancer Center Research Institute, Chiba 260-8717, Japan. [6]Core Research for Evolutional Science and Technology, Japan Science and Technology Agency, Saitama, 332-0012, Japan. [7]Division of Hematology/Oncology, Saitama Children's Medical Center, Saitama 339-8551, Japan. [8]Gunma Children's Medical Center, Shibukawa 377-8577, Japan.
*These authors contributed equally to this work.

©2008 Macmillan Publishers Limited. All rights reserved